

1 F. Adolphi & R. Muscheler: “Synchronizing the Greenland ice core and radiocarbon
2 timescales over the Holocene – Bayesian wiggle-matching of cosmogenic radionuclide
3 records”. Reply to Reviewers.

4
5 First of all we would like to thank both reviewers for their insightful and helpful comments.
6 Below we will address each comment point by point, showing the reviewers comments in
7 black and our response in blue. Changes to the original manuscript are highlighted in bold.
8 At the end of this file you will find a revised version of the manuscript with changes
9 highlighted in yellow.

10

11 **Reviewer #1:**

12 My overall assessment is that the treatment of the C-14 and Be-10 records is very
13 well done and that the transfer function will be extremely useful to the paleoclimate
14 community. The authors are experts on C-14 and Be-10 and I congratulate them on
15 applying their knowledge to this issue. I recommend publication in *Climate of the Past*
16 after some minor (but important) revisions and clarifications.

17 Thank you.

18 **General points**

19 **Climate influences on Be-10**

20 The discussion and treatment of climate influences on Be-10 is generally good, however
21 there are a few places where I think it could be improved:

22

23 PP2936, L13: It should be noted that most sites receive Be-10 from a combination of wet and
24 dry deposition processes. For example, the detailed treatment of wet and dry deposition
25 processes in the recent paper by Elsässer et al., [2015] suggests 32 (*?Apparently a part of the*
26 *original sentence was cut off here? We hope that our answer below addresses the question*
27 *correctly.*)

28

29 We agree. In fact, we address this point in line 15-16 (pp2936) by writing “While today wet
30 deposition is dominating over Greenland (Heikkilä et al., 2011) the ratio between wet and dry
31 deposition has likely changed over time (Alley et al., 1995).” Furthermore, by using
32 concentrations and fluxes separately, we account for both endmembers (wet/dry deposition)
33 of these processes. We show that these lead to consistent results (e.g., figure 5). Any mixing
34 between the two modes of deposition would hence, likely not change our results.

35 **We changed PP2936, L13 to:**

1 **“In reality, both modes of deposition contribute to the accumulation of ¹⁰Be on the ice**
2 **sheet. Today, wet deposition processes dominate over dry deposition which accounts for**
3 **about one third or less of the deposited ¹⁰Be in Greenland (Heikkilae et al., 2011,**
4 **Elsaesser et al. 2015). However, this dry/wet deposition ratio has likely been variable**
5 **over time (Alley et al., 1995).”**

6
7 PP2936, L18: Please add some more specific language on processes which
8 affect Be-10 concentration in ice e.g. revise to something like “: : Be-10 transport
9 paths, including stratosphere to troposphere exchange and air-mass precipitation
10 history and can cause climatic imprints...”

11
12 **We changed PP2936, L18 to: “Secondly, a variety of climatic influences can leave an**
13 **imprint in ice core ¹⁰Be records. Atmospheric circulation changes and air mass**
14 **precipitation history (i.e., ¹⁰Be scavenging by precipitation prior to the arrival of the air**
15 **mass at the ice core site) may, for example, modulate the transport path and efficiency**
16 **of ¹⁰Be delivery to the ice core site (Heikkilae & Smith 2013, Pedro et al. 2011, 2012).**
17 **Furthermore, changes in the exchange rates between stratospheric (high ¹⁰Be**
18 **concentrations) and the tropospheric (low ¹⁰Be concentrations) air masses can affect**
19 **the tropospheric ¹⁰Be budget (Pedro et al., 2011).”**

20
21 PP2936, L18: Elsässer et al., 2015 should be added to the list here, they suggest
22 a modest polar bias, similar to the results of Field et al.

23
24 **We added Elsaesser et al. 2015 to the reference list in PP2936, L 26-27.**

25
26 PP2942, L22: Note that the Pedro et al., result refers to the coastal East-
27 Greenland ice core site Das2 (not GRIP or GISP).

28
29 **Yes. However, we feel that PP2942, L17-23 should be seen as a short review of the range of**
30 **partly disagreeing results that have been published on the issue of a potential polar bias in**
31 **¹⁰Be records.**

32
33 PP2945:L5: The statement here assumes that the regression and linear detrending
34 with respect to other proxies in the ice core data does in fact remove all
35 centennial scale climate influences on Be-10. While I agree that the linear detrending
36 is a good step, it is not clear that it would remove all climate influence
37 on Be-10. For example, changes in stratosphere to troposphere exchange are
38 expected to influence Be-10 but not necessarily the other proxies that have been
39 used in the detrending. Please add something to the effect of “a caveat is that

1 climate influences specific to Be-10 will not be removed by the detrending technique”.

2
3 A good point. We changed PP2945, L3-6 to:

4 **“This is in agreement with Adolphi et al. (2014) who showed that centennial GRIP ¹⁰Be**
5 **variations are dominated by solar activity changes and indicate only little climatic**
6 **influences on ¹⁰Be sensitivity to the assumed mode of ¹⁰Be deposition even over large**
7 **deglacial climatic transitions. Other potential climatic influences on ¹⁰Be such as**
8 **changes in the stratosphere-troposphere exchange rates are, however, difficult to assess**
9 **from climate proxy data and will thus, not be removed by our detrending technique.”**

10
11 PP2945:L5: “little climatic influence on Be-10 even over large deglacial climatic
12 transitions”. This statement could be misinterpreted. It is well established that
13 glacial to interglacial climate transitions leave a very large imprint on Be-10,
14 mainly due to accumulation rate changes e.g. Finkel and Nishiizumi [1997].
15 Please revise the wording.

16
17 Agreed. We added:

18 **“It should be noted that this statement solely refers to the filtered centennial ¹⁰Be**
19 **variations investigated here.”**

20
21 PP2945, L3 and Figure 2. “The centennial changes in the GRIP and GISP2 Be-
22 ¹⁰ versions, however, are highly coherent and indicate a limited climate influence on Be-10
23 on these timescales”. Clarify if you refer to coherence between the
24 GISP2 and GRIP records or coherence internally within the GISP2 and GRIP
25 records. I would agree that there is good coherence between the curves from
26 the same site but it is not clear that there is good coherence between the records
27 from GRIP and GISP2. A panel in Figure 3 should be added to the main text
28 or at least to the review response showing the Be-10 concentration anomalies
29 at both GRIP and GISP2. The authors do not necessarily need to explain the
30 differences between the records but they should at least be acknowledged given
31 the statement “indicate a limited climate influence on Be-10 on these timescales”.
32 If the authors intend to say that there is good coherence between GRIP and
33 GISP2 records, it could help clarify the section to explain explicitly what is meant
34 by “coherence”, i.e. that the records share the main peaks but not the smaller
35 variations.

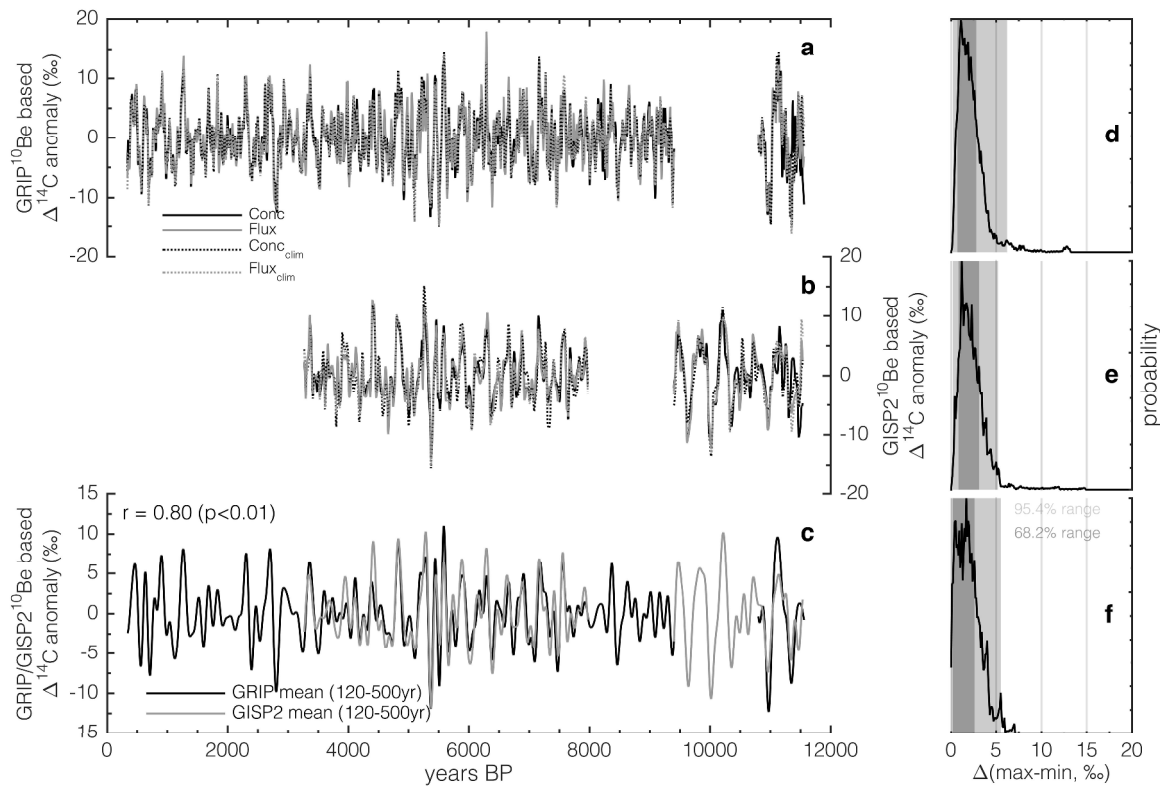
1 We changed figure 3 to the one shown below. To minimize the effect of sampling
 2 resolution differences we bandpass-filtered both records [120-500 yrs], i.e., the spectral
 3 band that is continuously resolved by both records.

4 We refer to this figure on P2945, L17:

5 “Similarly, the $\Delta^{14}\text{C}$ anomalies modelled from GRIP and GISP2 ^{10}Be agree within ± 2.5
 6 ‰ (figure 3, c, f).”

7 To further clarify that P2945, L1-3 refers to each ice core separately we changed it to:

8 “The centennial changes in the GRIP ^{10}Be versions, however, are highly coherent and
 9 indicate limited climate influence on these timescales and the same holds true for the
 10 GISP2 ^{10}Be versions.”



11
 12 Figure 3 (revised). Centennial (<500 years) $\Delta^{14}\text{C}$ variations modelled from GRIP and GISP2
 13 ^{10}Be data. Panels a and b show the modelled $\Delta^{14}\text{C}$ variations from ^{10}Be concentrations (solid
 14 black), fluxes (solid grey), “climate corrected” concentrations (dotted black), and “climate
 15 corrected” fluxes (dotted grey) for the GRIP (a) and GISP2 (b) ^{10}Be records. Panels d and e
 16 on the right side depict the probability density functions for the maximum $\Delta^{14}\text{C}$ difference
 17 between curves shown in panels a and b, respectively. Panel c shows the mean of all GRIP
 18 (black) and GISP2 (grey) ^{10}Be based $\Delta^{14}\text{C}$ anomalies shown in panels a and b, respectively.
 19 Panel f shows the corresponding probability density function of the maximum $\Delta^{14}\text{C}$
 20 differences. For this comparison both ice core records have been band-pass filtered [120 –

1 500 years] to minimize inconsistencies arising from their different sampling resolution. The
2 correlation between the GRIP and GISP2 records is given in panel c together with its p-value.

3

4 **Inferred C-14 production rates and IntCal13–GICC05 transfer function**

5 I will state up front that I do not have expertise in the Bayesian techniques used here
6 and hence I cannot critically review that aspect of the methodology. Nevertheless, I
7 have some questions and comments about the data treatment that I feel are important
8 to be addressed and which may help make the manuscript accessible to a wider
9 audience.

- 10 • PP2945 L17: Add a panel to Figure 3 showing the comparison between time
11 series of the GRIP and GISP based C-14 reconstructions. This would be useful
12 for the reader to see directly the coherence between the two, otherwise explain
13 why this direct comparison is not needed.

14 See above. We added a panel to figure 3.

15

16 The advantage and influence on uncertainty of going from 50 year $P_{S_{scaled}}$ to the
17 annual resolved final age transfer function could be better explained. It would
18 help to clarify how the interpolation affects the uncertainty if you could plot the $P_{S_{scaled}}(ts)$
19 (i.e on its 50 yr spacing) against the probability distributions for the
20 final age transfer function. The authors should address if the proposed Monte
21 Carlo method adds information compared to the simpler approach of interpolating
22 between the 95 (*?Again, something is missing here, but we assume it should read "...*
23 *between the 95% confidence intervals.*")

24

25 We do provide a direct comparison of $P_{S_{scaled}}(ts)$ to the transfer function in figure 9. The
26 approach to the transfer function is outlined in section 2.5. The key difference between $P_{S_{scaled}}$
27 and the transfer function is, that $P_{S_{scaled}}$ contains high-frequency variability in the derived
28 IntCal13-GICC05 difference which we do not believe we can reliably reconstruct. Since
29 $P_{S_{scaled}}$ is estimated on 1,000yr windows every 50 years, neighbouring windows contain about
30 95% of the same data. Hence, they cannot be used as independent likelihood estimates of the
31 timescale difference. To account for this oversampling each transfer function samples only
32 independent $P_{S_{scaled}}$ estimates (i.e., based on windows that are 1,000 years apart). Each
33 iteration of the MonteCarlo method starts from a randomly selected $P_{S_{scaled}}$ estimate and then
34 uses only every 20th window (i.e., one $P_{S_{scaled}}$ estimate per 1,000 years). Hence, every
35 individual transfer function has a lower sampling resolution than $P_{S_{scaled}}(ts)$ itself. Through
36 interpolation of the transfer functions to annual resolution, each likelihood estimate at each
37 point in time will consist of direct sampling of $P_{S_{scaled}}(ts)$ at this point in time as well as
38 interpolated values between neighbouring windows. This can be seen in figure 9 – the
39 transfer function is much smoother than $P_{S_{scaled}}(ts)$ but it encompasses the full range of
40 uncertainty. Consequently, the transfer function has larger uncertainty during periods where

1 P_{scaled} implies rapid changes in the timescale difference such as e.g. around 7-8 kaBP,
2 because we cannot reliably resolve the exact rate of change at this point.

3 Whether we interpolate the transfer functions to annual or 50yr resolution has no effect on the
4 uncertainty, and was merely done for practical reasons, i.e., to be able to provide an annual
5 transfer function to potential users.

6

7 Fig 9: The thin black lines are not defined (2-sigma on transfer function?). Also

8 please clarify the difference between the thin black lines and the $P_{\text{scaled}}(t)$. Why

9 do the $P_{\text{scaled}}(t)$ and transfer function deviate from each other in places (e.g.

10 7.5 to 8.0 ka). Is this the result of the 50-yr to annual Monte-Carlo interpolation,

11 which goes back to my question above?

12

13 Yes, these are the 2sigma intervals. **We changed the figure caption and legend of figure 9**
14 **accordingly.**

15 Regarding the disagreement between P_{scaled} and the transfer function we hope we could
16 explain the effect above.

17

18

19

20 P2948, eq. 4: The difference between the tree-ring and Be-10 based delta C-

21 14 values is sometimes zero (Fig. 7), and as the IntCal term is always positive,

22 the equality in eq. 4 is not satisfied. The statement may be true if using $<$ sign

23 instead. But the whole section appears a little convoluted. It seems to me that

24 what you do is to adjust the Be-10 scaling factor to minimize the (rms or rmsbinned)

25 difference between the tree-ring and Be-10-based Delta C-14 values.

26 After obtaining the best value of the scaling factor, you can use the rearranged

27 eq. 4 to estimate (what I would say is the lower bound of) the uncertainty of the

28 Be-10-based Delta C-14 values.

29

30 Good point. We agree, our previous formula was not complete and could be misinterpreted.

31 **Therefore, we clarified our method by including the rearranged equation 4 into the**
32 **main text:**

$$\partial(t)_{\text{Be}} = \sqrt{\partial(t)^2 - \partial(t)_{\text{IC}}^2}; \quad \partial(t) > \partial(t)_{\text{IC}}$$

33

$$\partial(t)_{\text{Be}} = 0; \quad \partial(t) \leq \partial(t)_{\text{IC}}$$

34

1 We think that this method is more appropriate than simply minimizing the RMSE between
2 ^{14}C and ^{10}Be , since it accounts for the fact that ^{14}C errors are increasing back in time due to
3 the relatively short half-life of ^{14}C .

4 We cannot evaluate whether this uncertainty estimate is a lower bound of the true
5 uncertainty, but it is the required error to bring ^{14}C and ^{10}Be into statistical agreement,
6 which is crucial for our methodology. However, to clarify that this uncertainty estimate is
7 only valid for the centennial (<500 year) variations in ^{10}Be -based $\Delta^{14}\text{C}$ we added to P2950,
8 L1-3:

9 “In conclusion we use a $^{14}\text{C} : ^{10}\text{Be}$ ratio of 1.1 : 1 and an uncertainty of 4‰ for the modelled
10 $\Delta^{14}\text{C}$ record to derive a final IntCal13-GICC05 transfer function in the next section. **It**
11 **should be noted that this uncertainty estimate is only valid for the centennial (<500**
12 **year) variations and the period studied here.”**

13
14 Section 2.2: Please specify whether you stretch or only shift the timescale of the
15 ice core Be-10 data to get an optimal fit with the IntCal C-14 data within each
16 1000-year window. This may be clear to those familiar with the Bronk Ramsey et
17 al. (2001) paper, but it would be good to make it explicit here.

18
19 We changed PP2940, L3 to: **“For each window we test for time scale differences (*shifts*) of**
20 **± 150 years *without stretching or compression of the time scale within this window.*”**

21
22 Section 2.2: The authors tests the method for robustness in many ways, but
23 the 1000-year width of the correlation window is not tested. That test should be
24 added or at least the authors should discuss why 1000 years is the best choice.

25
26 Good point. We did indeed test this effect.

27 We added on PP2940, L 4: **“We tested different window sizes between 500 and 2,000 year**
28 **length and the corresponding results are consistent within error. The choice of a 1,000**
29 **year window represents a trade-off between i) an increasing statistical robustness and**
30 **hence, smaller uncertainties, and ii) a loss of detail (variability) in the final transfer**
31 **function (see also section 2.5) with increasing window length.”**

32
33 Section around P2954, L4. Please note that the main part of the estimated IntCal13-GICC05
34 difference builds up during the period 8 – 10.3 ka BP, which is the section where the dating is
35 based on GRIP CFA data that have fewer components and lower resolution than the NGRIP
36 dataset employed from 10.3 ka BP downwards [Rasmussen et al., 2006]. The difference
37 curve (Figs. 9-11) levels out in the section between 10.3 ka BP and the onset of the Holocene,
38 corroborating that there are much smaller systematic counting errors in the section based on
39 NGRIP CFA data.

40
41 Yes this is correct. We feel that we do point this out in P2954, L 3-6 where we write:

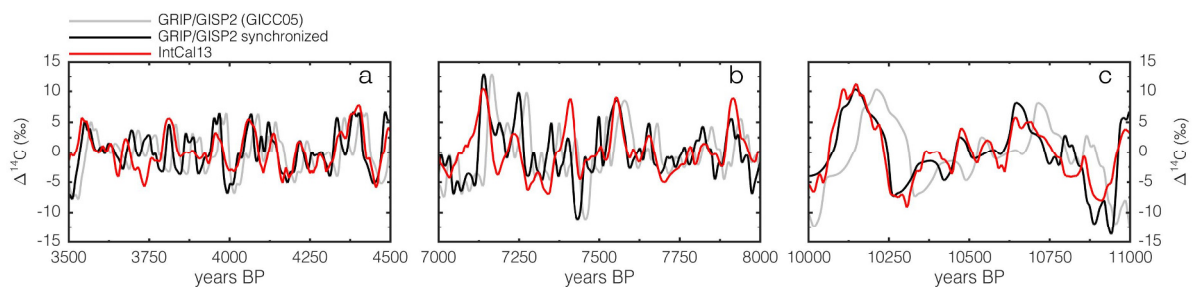
1 “It can, however, not be assumed that the counting error continues to be systematic beyond
2 this period, since the parameters used for layer identification as well as the sources of
3 uncertainty (e.g. melt layers) differ back in time under changed climatic conditions
4 (Rasmussen et al., 2006).”

5
6 Fig 7 and Section 2.2 and 2.5: The fit is very impressive. It would be help the
7 reader to see how your method has reduced uncertainly between the timescales
8 if you could also show some comparisons before synchronisation. I would suggest
9 to show at least one, and preferably 2-3 examples (e.g. best, typical, worst)
10 of 1000-year long sections of wiggle-matched records to allow the reader to evaluate
11 the robustness of the fit.

12
13 **We added Figure 10 to section 3.4** (see below). We picked the sections between 3,500 –
14 4,500 BP (a section of relatively low amplitude $\Delta^{14}\text{C}$ changes, i.e., the variations are close to
15 the estimated 10Be RMSE), between 7,000-8,000 BP (i.e. a section with larger $\Delta^{14}\text{C}$
16 variations, but not continuously good agreement between 10Be and 14C), and 10,000-11,000
17 BP (i.e. a section with large $\Delta^{14}\text{C}$ variations and a near perfect fit between 10Be and 14C).

18 We expanded the main text on P2950 (L18 onwards):

19 **“Figure 10 shows three examples of GRIP 10Be based $\Delta^{14}\text{C}$ anomalies before (grey) and
20 after (black) synchronization to IntCal13 (red). The examples encompass (i) a period of
21 relatively low $\Delta^{14}\text{C}$ variability ($\pm 5\text{-}7\%$) but good agreement between GRIP and
22 IntCal13 (figure 10, a), (ii) a period of large $\Delta^{14}\text{C}$ variability ($\pm 10\%$) but less good
23 agreement between GRIP and IntCal13 (figure 10, b), and (iii) a section of large $\Delta^{14}\text{C}$
24 ($\pm 10\%$) variability and excellent agreement between GRIP and IntCal13 (figure 10, c).
25 It can be seen, that in all cases the fit between GRIP and IntCal13 is improved when
26 applying the proposed GICC05-IntCal13 transfer function. However, figure 10 (b) also
27 shows, that short periods of disagreement (i.e., around 7,250 – 7,500 years BP) may
28 remain, as they cannot be reliably resolved by our method which matches 1,000 year-
29 long sections. It should, however, be noted that matching these short sections would i)
30 represent a serious violation of the GICC05 counting error which is minimal over these
31 short periods of time (± 6 years at 2σ between 7,250 – 7,500 years BP), and ii) not
32 account for the possibility that 10Be and 14C may simply not agree due to the caveats
33 outlined in the introduction. Furthermore, the applied shift of GICC05 in figure 10 (b)
34 leads to an improved agreement between 14C and 10Be after and prior to 7,250 and
35 7,500, respectively. Hence, we consider it unlikely that for this short period of time the
36 timescale difference deviates significantly from the estimate for the entire window.”**



37

1 Figure 10. GRIP/GISP2 ^{10}Be based $\Delta^{14}\text{C}$ before (grey) and after (black) synchronization to
2 IntCal13 (red) for the sections a) 3,500-4,500 years BP, b) 7,000-8,000 years BP, c) 10,000-
3 11,000 years BP.

4

5 In the final version please specify where the IntCal13–GICC05 transfer function
6 (and relative and absolute uncertainties) will be made available.

7

8 We will provide the transfer function as a supplementary file to this paper and on NOAA.

9

10 PP2953, L15-20: Worth to specify that the difference is in the direction of systematic
11 over-counting of years.

12

13 We added on P2953, L17: “...(i.e., a systematic over-counting of years).”

14

15 **Technical points**

16 • Many of the figures have multiple lines overlain that become hard to distinguish,
17 e.g Fig 5 has 4 lines plus shading. Use of color would probably improve clarity.

18 The figures also appear small. I had to zoom in on the screen to see important
19 details. Can you make the figures bigger?

20

21 We added color to the lines in Figure 5. Regarding the size of the figures: We will provide
22 them in full A4 size.

23

24 In general, ‘both’ is overused. When it is clear that you are talking about two
25 things it is mostly not needed to say both. An example: PP2945, “Both, changes in ocean
26 ventilation [and] air–sea gas-exchange can cause $_{\text{C}}\text{-14}$ anomalies

27 larger than the amplitude of $_{\text{C}}\text{-14}$ anomalies induced by C-14 production rate

28 changes only”. Drop the “both”, it only confuses things here. Also: “One method

29 to compare and synchronize both timescales is the use of cosmogenic radionuclide
30 records”. Here, “both” is misleading unless you are synchronizing (both)

31 time scales to a third one.

32

33 Agreed. We reworked the use of “both” carefully.

34

35 P2935, L22: “ideal tool” is overstating things given the climate and carbon cycle
36 influences.

1
2
3
4
5
6
7
8
9
10
11
12
13
14
15
16
17
18
19
20
21
22
23
24
25
26
27
28
29
30
31
32
33
34
35
36
37

We exchanged “ideal” with “powerful”.

P2936, L11: Delete “On the other hand”.

Done.

Section 2.2: Typos: Bronk not Bonk.

Fixed.

Please state what dating of GISP2 was used: obviously it should be GISP2 on GICC05.

On P2938, L7, we added: “We used the GISP2 ¹⁰Be record on the GICC05 timescale (Seierstad et al. 2014).”

Figure 1 Caption: Key data not Key-data. I also noticed some other examples of funny use of hyphens. Please check usage throughout.

Changed figure 1 figure caption and we will check the rest of the manuscript for similar mistakes.

Figure 2 Caption: I can’t make sense of the second last line, please revise.

Ok. Actually this sentence may not be necessary at all, since we discuss the differences between the different ¹⁰Be versions (concentrations, fluxes, climate corrections) later on in Figure 3 and the corresponding text sections. We deleted this sentence from the figure caption.

Figure 5 caption: Description of panel b) appears to be referring to an earlier version.

No, this is indeed the correct caption. To clarify: The patch shows probabilities based on GRIP ¹⁰Be, where gaps in the GRIP record have been filled using GISP2 ¹⁰Be data. Hence, GISP2 can only be used as an independent validation where GRIP and GISP2 have

1 overlapping ^{10}Be data. The 95% confidence intervals based on GISP2 ^{10}Be during these
2 overlapping sections is plotted as lines in comparison to the patch, which is the same in all
3 panels (GRIP ^{10}Be with GISP2 ^{10}Be filling the gaps). We hope that this is clear from the first
4 5 lines of the figure caption as well as from P2946, L20-22.

5
6 Note some inconsistency in x-axis labels: sometimes yrs BP and sometimes
7 years BP.

8
9 **Changed consistently to “years BP”.**

10
11 Add space between ka and BP, eg on PP2947.

12
13 **Done.**

14
15 **Anonymous Referee #2**

16 The manuscript is well-written and easy to follow. The authors have great attention
17 for detail, which results in realistic uncertainty estimates that reflect all the probable
18 causes of uncertainty.

19
20 **Thank you.**

21
22 My only concern is that it's hard to discern what is really new
23 here. A very similar paper was published last year by the same authors (Muscheler,
24 Adolphi and Knudsen, 2014), MAK14 hereafter. The manuscript under review uses the
25 same ^{10}Be and D14C data as MAK14, and while the mathematical details differ, the
26 approach is conceptually identical (i.e. converting ice-core ^{10}Be to ^{14}C using a carboncycle
27 model, and then wiggle-matching it to IntCal D14C). Unsurprisingly, the transfer
28 function the authors derive is essentially identical to the one derived by MAK14 – only
29 smoother due to the choice of a 1000 year window length. The main improvement is a
30 reduction in the uncertainty estimates, suggesting that MAK14 were too conservative
31 in estimating their error.

32 **The aim of this manuscript is twofold.**

33
34 1. We present a novel approach to synchronize radionuclide records from different archives
35 that is applicable to a multitude of records. We anticipate that the methodology itself will be
36 applied in further studies, and hence, we describe in detail its underlying assumptions and

1 caveats. In addition to MAK14 we also test our results using different ^{10}Be records (GRIP
2 and GISP2) to illustrate the robustness of our results and methodology. Furthermore, we
3 assess uncertainties arising from the geochemistry of ^{10}Be and ^{14}C explicitly which is a
4 significant improvement compared to MAK14 which also has general implications for the
5 interpretation of these records (i.e. for solar activity reconstructions). Hence, we think we can
6 provide a significant conceptual advance on how to link cosmogenic radionuclide records and
7 lie out a framework that will be of great value for future studies.

8
9 2. We provide a transfer function between GICC05 and IntCal13 for the Holocene. Compared
10 to MAK14 this function is less (not more, see figure 7 in MAK14) smooth than the proposed
11 transfer function of MAK14 which is based on a 2,000 year window. More importantly, we
12 do not only provide smaller, but also more robust uncertainty estimates on the transfer
13 function (which we have to acknowledge were not satisfactorily defined in MAK14). This is
14 a significant improvement as reliable uncertainty estimates are crucial if the transfer function
15 shall be applied to determine robust leads and lags in the climate system between ice core and
16 radiocarbon dated paleoclimate records.

17 We clarified the value of this publication with respect to MAK14 by modifying the abstract
18 to:

19 **„Compared to earlier work, we employ a novel statistical approach which leads to**
20 **strongly reduced and yet, more robust, uncertainty estimates. Furthermore, we**
21 **demonstrate that the inferred timescale differences are robust independent of (i) the**
22 **applied ice core ^{10}Be records, (ii) assumptions of the mode of ^{10}Be deposition, as well as**
23 **(iii) carbon cycle effects on ^{14}C , and (iv) in agreement with independent estimates of the**
24 **timescale differences.“**

25 In addition, section 1.1 (aim of this study) refers to the advantages of the proposed method
26 and tests as compared to MAK14.

27
28 The work is very thorough, and I have only a few minor comments that should be
29 addressed in a revised manuscript. I leave out the first two digits (“29”) in all listed
30 page numbers.

31
32 - I think section 2.2 (statistical method) would fit more logically between the current
33 sections 2.4 and 2.5. When reading the section on the statistical method, the reader
34 has no idea what is meant by “ ^{10}Be -based D^{14}C anomalies” (P38, last line). This
35 becomes clear after reading section 2.4. An alternative solution would be to add an
36 introductory paragraph to section 2.2 in which the conceptual framework is laid out, so
37 the reader understands that ^{10}Be is converted to ^{14}C using a carbon cycle model, and
38 then filtered to isolate the centennial component.

39
40 This is a good point. We added an introductory paragraph to section 2.2:

1 “In the following section we will describe the statistics involved in the $^{14}\text{C}/^{10}\text{Be}$
2 comparison. To be able to compare both radionuclides quantitatively, we converted the
3 ice core ^{10}Be records into $\Delta^{14}\text{C}$ variations using a box-diffusion carbon cycle model
4 (Siegenthaler et al., 1980; Muscheler et al., 2004b). The details of this conversion and its
5 uncertainties are addressed in more detail in section 2.4. In the following we will refer to
6 the modelled $\Delta^{14}\text{C}$ variations as „ ^{10}Be -based $\Delta^{14}\text{C}$ anomalies“.”

7
8
9 - Due to their proximity, the GISP2 and GRIP sites should experience identical atmospheric
10 ^{10}Be loading; yet GISP2 receives slightly more accumulation than GRIP (about
11 5%). Could this help in partitioning out wet and dry ^{10}Be deposition? The lower ^{10}Be
12 concentrations at GISP2 (by 0.12 atoms/g), as well as the higher $^{14}\text{C}/^{10}\text{Be}$ scaling
13 factors (Figs 6 and 7) are both consistent with a fraction of dry deposition. I fear that
14 the accumulation difference may be too small to do this reliably, though.

15
16 This is an interesting thought. However, to assess this reliably a detailed evaluation of the
17 ^{10}Be concentration / ice accumulation rate relationship would be required. For the purpose of
18 clarity of the manuscript we would prefer not to discuss this issue extensively. We show, that
19 GRIP and GISP2 ^{10}Be records yield similar synchronization results to IntCal13 (figure 5, b).
20 Furthermore, ^{10}Be concentrations and fluxes give consistent synchronization estimates
21 (figure 5, a) indicating that the assumed mode of ^{10}Be deposition is of minor importance for
22 the results of this study. Regarding the slightly different ^{10}Be scaling factors of GRIP and
23 GISP2 records (figure 7), we think that this difference should not be over-interpreted. The
24 GISP2 ^{10}Be record has a lower sampling resolution and a slightly higher scaling factor may
25 just result from this difference in smoothing. Last but not least, due to slight differences in the
26 ^{10}Be sample preparation of both ice cores (see Finkel and Nishiizumi 1997, JGR) we cannot
27 exclude that the small difference in the ^{10}Be concentration reflects an interlaboratory
28 difference.

29
30 - Section 2.1: please indicate the data resolution for the $\Delta^{14}\text{C}$ data also.

31 We added in P2938, L18: “...and presented in IntCal13 in 5-year resolution while the
32 underlying data has typically a resolution of 10 years for most of the Holocene”

33
34 - P37 L1-L4: I think the reality is more fluid than portrayed. I suspect that in practice
35 the ^{10}Be - ^{14}C synchronization is dominated by a few prominent events, and therefore
36 somewhat “discrete”. Likewise, continuous (rather than discrete) CH_4 synchronization
37 has also been achieved between ice cores (Mitchell et al., Science 342 964-966, 2013).

1 We think that a strength of the methodology applied here lies in its lower sensitivity to single
2 events than the methodology of MAK14. The methodology of MAK14 is based on
3 correlation analysis, which relies on the covariance of two records. Hence, this type of
4 analysis can be dominated by single events of large amplitudes. In comparison, the
5 methodology applied in the manuscript presented here does compare $^{14}\text{C}/^{10}\text{Be}$ data pairs in
6 a reduced Chi^2 -like fashion. I.e., the values are compared directly irrespective of their
7 covariance. This allows for example also to exploit the information “a 500 year long section
8 of zero D^{14}C anomaly” – while the covariance of such a section would be zero. Therefore,
9 common variability as well as common non-variability go with similar weight into the
10 comparison. Obviously, D^{14}C anomalies are needed to achieve a synchronization and (in the
11 example above) constrain the length of a section with small D^{14}C anomalies. And we agree,
12 that a slight dominance of these larger D^{14}C anomalies can be expected, since these
13 anomalies will exceed the uncertainty of the $^{14}\text{C}/^{10}\text{Be}$ records, maximizing equation 1.
14 However, as outlined above we do think, that also relatively “flat” sections of $^{14}\text{C}/^{10}\text{Be}$
15 contribute significantly to the synchronization i.e. we evaluate all available information.

16 **To tone down our statement in P2937, L 1-4, and also with respect to the findings by**
17 **Mitchell et al. (2013), we changed P2937, L 1-4 to:**

18 **“... has the advantage that it can provide near-continuous estimates of the time scale**
19 **differences [...] or changes in atmospheric trace gases during Dansgaard-Oeschger**
20 **events.”**

21

22 - P40, L25: “....and may thus diminish the climate influences in the ^{10}Be record”. Could
23 it also increase the climate influences in the ^{10}Be record, if the observed correlations
24 are spurious?

25

26 Yes, in theory this could happen. However, the removed correlations were indeed significant.
27 In addition, we hope we explain sufficiently well on P2940 (L26) – P2941 (L5) that these
28 corrections are not meant to be interpreted as improved “climate free” versions of the ^{10}Be
29 records, but as sensitivity tests to our methodology.

30

31

32 - Section 2.4.1: What is the motivation to only investigate the sensitivity of the model
33 to the oceanic carbon exchange? While the ocean is of course the largest carbon
34 reservoir, the terrestrial carbon fluxes are actually larger than the oceanic ones. A
35 recent paper also suggested that changes in terrestrial carbon reservoirs are more
36 important during Holocene (Bauska et al. Nat Geo 8, 383-387 2015)

37 We agree that terrestrial carbon fluxes are a major component in the global carbon cycle.
38 However, due to the short turnover rate of the terrestrial biosphere, the biologically stored
39 carbon has essentially the same ^{14}C signature as the atmosphere. Hence, changes in the
40 biosphere – atmosphere CO_2 exchange, do not exert a strong control on atmospheric ^{14}C
41 concentrations (i.e. a large flux of terrestrial carbon won't change the $^{14}\text{C}/^{12}\text{C}$ ratio in the
42 atmosphere significantly).

1
2
3
4
5
6
7
8
9
10
11
12
13
14
15
16
17
18
19
20
21
22
23
24
25
26
27
28
29
30
31
32
33
34
35
36
37
38
39

- Section 2.6: I think it's important somewhere to point out that you're comparing the 14C anomalies, rather than 14C itself. These anomalies are not really well defined; from section 3.1 I assume you're using the centennial (<500 yr) variations. Please describe how you filter the records to separate the <500 and >500 yr variations.

We explain in section 2.2 (P2938, L23-26) why we use D14C anomalies rather than absolute values or 14C-ages. We consider the use of a 500 year high-pass filter a result rather than part of the method as it results from the climate and carbon cycle related 10Be uncertainties (section 3.1) which are timescale dependent and minimize for these short wavelengths.

We specified more clearly on P2946, L13:

“In the following we will compare the centennial (i.e., <500 years separated by an FFT-based High-Pass filter) D14C anomalies as reconstructed from tree-rings (IntCal13) and ice cores (GRIP/GISP2 10Be-based) with respect to their timescale differences. The choice of a 500 year high-pass filter results from the climate and carbon cycle related uncertainties shown in section 3.1 which increase on longer timescales.”

- P45, L16-17: How much is the uncertainty of 3 ‰ relative to the standard deviation of the data itself? In other words, what is the signal to noise ratio?

The standard deviation of the GRIP 10Be based D14C record is 4.5 per mille, yielding a signal to noise ratio of ca. 1.5. We'd like to point out that the uncertainty estimate is very conservative since we treat the climate influence on 10Be as a systematic uncertainty (i.e., Figure 3 shows the difference between the maximum and minimum D14C value at each point in time, as opposed to the standard deviation of all 10Be versions).

- P48, L21: “this would imply a strong polar bias”. Please elaborate, this is not automatically clear.

We introduce and discuss the issue of a polar bias in the introduction and in section 2.4.2.

To make it more clear we changed L21 on P2948 to: **“Assuming that the centennial 10Be and 14C production rate changes are mainly modulated through solar activity this low scaling factor would point to a strong polar bias of the GRIP GISP2 10Be records (see sections 1 and 2.4.2).**

- The generated transfer function should be provided as a text / excel file in the supplement.

Yes, it will be.

1
2
3
4
5
6
7
8
9
10
11
12
13
14
15
16
17
18
19
20
21
22
23
24
25
26
27
28
29
30
31
32
33
34

- Typos / Language:

P35 L15 and throughout: acronym should be capitalized, so GCR instead of gcr.

Done.

P36, L4: 14C / 12C *ratio*

Added.

P38, L23: Please define what is meant by “D14C anomalies”. I don’t think this is done anywhere in the manuscript.

We define D14C on P2938, L16 and think that the term “anomalies” is a general term that describes deviations from a mean. As outlined above, we think that the use of centennial anomalies (i.e., deviations from a 500 year low-pass filtered D14C record) is a result of section 3.1, which may partly differ if the method was applied to a different 10Be record, with different climate influences. We do outline on P2938, L23-26 why absolute D14C values cannot be used and hope that our definition of anomalies becomes clear throughout the manuscript and with the additions on P2946, L13 (see above).

To increase the clarity of the manuscript we added on P2938, L 26:

“Given the results shown in section 3.1 we employ centennial (<500 year high-pass filter) $\Delta^{14}\text{C}$ anomalies of the tree-ring and the 10Be-based $\Delta^{14}\text{C}$ records for this comparison as shown in figure 3.”

P39, L4 and L8: Bronk Ramsey (“r” omitted)

Fixed.

Throughout there are long sentences that would benefit from inclusion of a comma to clarify sentence structure. Some examples:

P35 L23: After production, ... P36 L11: On the other hand, ... P36 L28: ... synchronization tools, ... P40 L19: ... to the ice sheet, ... P41 L18: ... these effects, ... P45 L26: ... as before, ...

Reworked.

Synchronizing the Greenland ice core and radiocarbon timescales over the Holocene - Bayesian wiggle-matching of cosmogenic radionuclide records

F. Adolphi¹ and R. Muscheler¹

[1]Department of Geology – Quaternary Science, Lund University, Sweden

Correspondence to: F. Adolphi (Florian.Adolphi@geol.lu.se)

Abstract

Investigations of past climate dynamics rely on accurate and precise chronologies of the employed climate reconstructions. The radiocarbon dating calibration curve (IntCal13) and the Greenland ice core chronology (GICC05) represent two of the most widely used chronological frameworks in paleoclimatology of the past ~50,000 years. However, comparisons of climate records anchored on these chronologies are hampered by the precision and accuracy of both timescales. Here we use common variations in the production rates of ^{14}C and ^{10}Be recorded in tree-rings and ice cores, respectively, to assess the differences between both timescales during the Holocene. Compared to earlier work, we employ a novel statistical approach which leads to strongly reduced and yet, more robust, uncertainty estimates. Furthermore, we demonstrate that the inferred timescale differences are robust independent of (i) the applied ice core ^{10}Be records, (ii) assumptions of the mode of ^{10}Be deposition, as well as (iii) carbon cycle effects on ^{14}C , and (iv) in agreement with independent estimates of the timescale differences. Our results imply that the GICC05 counting error is likely underestimated during the most recent 2,000 years leading to a dating bias that propagates throughout large parts of the Holocene. Nevertheless, our analysis indicates that the GICC05 counting error is generally a robust uncertainty measurement but care has to be taken when treating it as a nearly Gaussian error distribution. The proposed IntCal13-GICC05 transfer function facilitates the comparison of ice core and radiocarbon dated paleoclimate records at high chronological precision.

1 1 Introduction

2 Paleoclimatology can provide significant insights into natural climate changes and thus,
3 improve our understanding of the climate system. Besides the reconstruction of past climate
4 itself, a precise chronology of each paleoclimate record is crucial to reliably assess the
5 dynamics of the inferred changes. Furthermore, consistent chronologies across multiple
6 paleoclimate records are required to assess the spatiotemporal evolution of climatic events
7 and thus, to test for potential leads and lags within the climate system and ultimately improve
8 the understanding of the underlying processes of past climate change. Two independent key
9 timescales in paleoclimatology of the past 50,000 years are the radiocarbon- (IntCal13,
10 Reimer et al., 2013) and the Greenland ice core timescale (GICC05, Andersen et al.,
11 2006;Rasmussen et al., 2006;Seierstad et al., 2014;Svensson et al., 2008;Vinther et al., 2006).
12 To be able to infer leads and lags between paleoclimatic changes anchored on these
13 chronologies at high precision, it is crucial to test the consistency between the timescales and
14 establish climate-independent isochrones and thus, reduce the influence of their absolute
15 dating uncertainties (e.g., Lane et al., 2013). One method to compare and synchronize
16 different timescales is the use of cosmogenic radionuclide records, such as ^{10}Be and ^{14}C
17 (Muscheler et al., 2014a;Muscheler et al., 2014b;Muscheler et al., 2008;Southon, 2002).

18 Cosmogenic radionuclides such as ^{10}Be and ^{14}C are produced in the atmosphere through a
19 nuclear cascade mainly triggered by incoming galactic cosmic rays (GCR, Lal and Peters,
20 1967). The flux of GCR reaching the atmosphere is in turn modulated by the strength of the
21 helio- and geo- magnetic fields resulting in varying production rates of ^{10}Be and ^{14}C (Masarik
22 and Beer, 2009, 1999;Kovaltsov et al., 2012;Kovaltsov and Usoskin, 2010). Thus, increased
23 (decreased) intensity of the solar- and/or geomagnetic field will result in decreased
24 (increased) cosmogenic radionuclide production rates. Therefore, ^{14}C and ^{10}Be production
25 rates co-vary globally due to external processes, making them a **powerful** synchronization
26 tool.

27 After production, ^{14}C oxidizes to $^{14}\text{CO}_2$ that enters the global carbon cycle and gets stored in
28 various environmental archives such as tree rings, sediments, and speleothems. ^{10}Be attaches
29 to aerosols which are deposited within 1-2 years (Raisbeck et al., 1981) by wet and dry
30 deposition processes and is stored in sediments including polar ice sheets. These ‘system
31 effects’ (i.e., non-production influences on ^{10}Be and ^{14}C records such as the mixing, transport,
32 and deposition of ^{14}C and ^{10}Be) can challenge an unequivocal reconstruction of cosmogenic

1 radionuclide production rates from paleoarchives and thus, synchronization efforts based on
2 cosmogenic radionuclides.

3 Due to the large actively exchanging carbon reservoirs, changes in the atmospheric $^{14}\text{C}/^{12}\text{C}$
4 ratio are attenuated and delayed compared to the corresponding ^{14}C production rate variations
5 (Oeschger et al., 1975). In comparison, ^{10}Be is a more direct recorder of production rate
6 changes. Thus, when comparing ^{14}C and ^{10}Be records directly, this difference in
7 geochemistry has to be taken into account by using carbon cycle models (Muscheler et al.,
8 2004b). However, to be fully realistic, these corrections would require prior knowledge on
9 the variable state of the carbon cycle, which is often difficult to quantify (Köhler et al., 2006).

10 ^{10}Be records (for example from ice cores) can be affected by non-production related
11 processes as well. Firstly, it depends on the assumed mode of deposition (wet vs. dry)
12 whether the ^{10}Be concentration (all wet deposition) or the ^{10}Be flux (all dry deposition) is the
13 better measure of atmospheric ^{10}Be concentration changes (Alley et al., 1995; Delaygue and
14 Bard, 2010). In reality, both modes of deposition contribute to the accumulation of ^{10}Be on
15 the ice sheet. Today, wet deposition processes dominate over dry deposition which accounts
16 for about one third or less of the deposited ^{10}Be in Greenland (Heikkilä et al., 2011; Elsässer
17 et al., 2015). However, this dry/wet deposition ratio has likely been variable over time (Alley
18 et al., 1995). Secondly, a variety of climatic influences can leave an imprint in ice core ^{10}Be
19 records. Atmospheric circulation changes and air mass precipitation history (i.e., ^{10}Be
20 scavenging by precipitation prior to the arrival of the air mass at the ice core site) may, for
21 example, modulate the transport path and efficiency of ^{10}Be delivery to the ice core site
22 (Heikkilä and Smith, 2013; Pedro et al., 2012; Pedro et al., 2011b). Furthermore, changes in
23 the exchange rates between stratospheric (high ^{10}Be concentrations) and the tropospheric
24 (low ^{10}Be concentrations) air masses can affect the tropospheric ^{10}Be budget (Pedro et al.,
25 2011a). Thirdly, contrary to ^{14}C , ^{10}Be might not be hemispherically well mixed owing to its
26 short atmospheric residence time. This has led to the proposition of a so-called “polar bias” in
27 ice core ^{10}Be records, stating that if polar ^{10}Be records were dominated by ^{10}Be produced at
28 high latitudes, the anisotropy of the geomagnetic shielding would lead to an enhanced solar-
29 and an attenuated geomagnetic modulation signal in polar ^{10}Be records. There is
30 contradicting evidence from data and modelling studies to whether this is the case (Field et
31 al., 2006; Bard et al., 1997; Pedro et al., 2012; Muscheler and Heikkilä, 2011; Heikkilä et al.,
32 2009; Elsässer et al., 2015).

1 In summary, to be able to use ^{10}Be and ^{14}C as synchronization tools, ‘system effects’ on each
2 radionuclide have to be assessed and corrected for. If successful, this method has the
3 advantage that it can provide near-continuous estimates of time scale differences as opposed
4 to discrete tie-points obtained from tephrochronology (Abbott and Davies, 2012; Lane et al.,
5 2013) or changes in atmospheric trace gases during Dansgaard-Oeschger events (Blunier et
6 al., 1998; Buizert et al., 2015).

8 1.1 Aim of this study

9 Recently, Muscheler et al. (2014a) assessed the differences of the radiocarbon and ice core
10 time scales for the past 14,000 years by comparing GRIP ^{10}Be (Yiou et al., 1997; Muscheler et
11 al., 2004b; Vonmoos et al., 2006) and IntCal13 ^{14}C data (Reimer et al., 2013). Here, we revisit
12 this approach using a different statistical framework (Bronk Ramsey et al., 2001) that is
13 computationally less expensive and provides improved error estimates for the inferred
14 timescale differences as compared to the method used in Muscheler et al. (2014a).
15 Furthermore, we test the robustness of the obtained results with respect to the use of different
16 ice core ^{10}Be records as well as potential ‘system effects’ on the radionuclide records. We
17 focus our analysis on the period where dendrochronologically dated high quality ^{14}C
18 measurements on tree rings are available. While this is theoretically the case back to 12,560
19 calBP (calibrated before present, AD1950, Friedrich et al., 2004), the accuracy of the oldest
20 part of tree-ring chronology has recently been questioned (Hogg et al., 2013) causing a gap in
21 the ^{14}C records underlying IntCal13 around 12,000 calBP (Reimer et al., 2013). Hence, we
22 limit our analysis to the Holocene where dendrochronological and ^{14}C -data replication is high
23 and most robust (Reimer et al., 2013; Friedrich et al., 2004).

25 2 Methods

26 2.1 Data

27 The key data used in this paper is shown in figure 1. The GRIP ^{10}Be record (Vonmoos et al.,
28 2006; Muscheler et al., 2004b; Yiou et al., 1997) covers almost the entire Holocene with a gap
29 between 9,400 and 10,800 years BP (Before Present 1950 AD) and no data for sections
30 younger than 300 years BP. We use the data as presented in Vonmoos et al. (2006) that

1 includes a 61-point binomial filter (roughly corresponding to a 20 year low-pass filter or a
2 decadal sampling resolution) minimizing weather related noise in the ^{10}Be data. The GISP2
3 ^{10}Be record (Finkel and Nishiizumi, 1997) has a gap between 7980 and 9400 years BP and no
4 data for sections younger than 3270 years BP. We used the GISP2 ^{10}Be record on the
5 GICC05 timescale (Seierstad et al., 2014). Its temporal resolution varies between 20 to 60
6 years with an average of one sample every 35 years. Hence, no smoothing filter was applied.
7 The GISP2 ^{10}Be concentrations have been normalized to the same standard used for the GRIP
8 ^{10}Be measurements (NIST SRM 4325, see Yiou et al., 1997; Muscheler et al., 2004b). The
9 resulting GRIP and GISP2 ^{10}Be records differ by on average $0.12 \cdot 10^4$ atoms/g of ice. To avoid
10 inhomogeneities when splicing the records together, we adjusted the GISP2 ^{10}Be data
11 accordingly by adding $0.12 \cdot 10^4$ atoms/g to the GISP2 ^{10}Be record (see figure 1). We note that
12 reconciling the ^{10}Be records through normalization instead of addition does not affect the
13 results shown here. The lower panel in figure 1 shows atmospheric $\Delta^{14}\text{C}$ (that is $^{14}\text{C}/^{12}\text{C}$ after
14 correction for fractionation and decay relative to a standard) as reconstructed from
15 dendrochronologically dated tree rings (Friedrich et al., 2004) and presented in IntCal13 in 5-
16 year resolution while the underlying data has typically a resolution of 10 years for most of the
17 Holocene (Reimer et al., 2013).

18

19 2.2 Statistical method

20 In the following section we will describe the statistics used for the $^{14}\text{C}/^{10}\text{Be}$ comparison. To
21 be able to compare both radionuclides quantitatively, we converted the ice core ^{10}Be records
22 into $\Delta^{14}\text{C}$ variations using a box-diffusion carbon cycle model (Siegenthaler et al.,
23 1980; Muscheler et al., 2004b). The details of this conversion and its uncertainties are
24 addressed in more detail in section 2.4. In the following we will refer to these modelled $\Delta^{14}\text{C}$
25 variations as „ ^{10}Be -based $\Delta^{14}\text{C}$ anomalies“.

26 We employ a statistical approach that is commonly used in the ‘wiggle-match dating’ of ^{14}C
27 records that have an initial relative chronology, i.e. the age differences between neighbouring
28 samples are known, such as tree-rings (Bronk Ramsey et al., 2001). Contrary to classical ^{14}C -
29 age calibration we use $\Delta^{14}\text{C}$ anomalies, since ^{10}Be cannot provide information on absolute
30 $\Delta^{14}\text{C}$ (and hence, ^{14}C -ages) which depends on ^{14}C production rates and the state of the carbon
31 cycle long before the investigated period. Given the results shown in section 3.1 we employ
32 centennial (<500 year FFT high-pass filter) $\Delta^{14}\text{C}$ anomalies of the tree-ring and the ^{10}Be -

1 based $\Delta^{14}\text{C}$ records for this comparison as shown in figure 3. The mathematical formulation
 2 remains however, unchanged. The calibration record, IntCal13 (Reimer et al., 2013),
 3 describes $\Delta^{14}\text{C}$ anomalies for each point in time, $R(t)$, with an associated uncertainty, $\delta R(t)$.
 4 This can be compared to ^{10}Be -based $\Delta^{14}\text{C}$ anomalies ($R_{i:n}$) for which we know the absolute
 5 age differences (Δt_i) between each sample from ice core layer counting. We can estimate the
 6 probability (P_i) for different assumed time scale differences between the records (t_s) for each
 7 sample by using equation 8 in Bronk Ramsey et al. (2001):

$$8 \quad P_i(t_s + \Delta t_i) \propto \frac{\exp\left(-\frac{(R_i - R(t_s + \Delta t_i))^2}{2(\delta R_i^2 + \delta R^2(t_s + \Delta t_i))}\right)}{\sqrt{\delta R_i^2 + \delta R^2(t_s + \Delta t_i)}} \quad (1)$$

9 Using Bayes' theorem to combine the probabilities for each individual measurement we can
 10 obtain an overall probability (P_s) for each time scale difference between GICC05 and
 11 IntCal13 (equation 9 in Bronk Ramsey et al., 2001):

$$12 \quad P_s(t_s) \propto \prod_{i=1}^n P_i(t_s + \Delta t_i) \quad (2)$$

13 To allow a continuous comparison, all records have been interpolated to annual resolution.
 14 However, since the ice core sampling resolution is in reality lower we do not obtain truly
 15 independent probability distributions for each sample. Consequently, we correct for the
 16 reduced degrees of freedom by scaling P_s as:

$$17 \quad P_{s_{scaled}}(t_s) = P_s(t_s)^{1/r} \quad (3)$$

18 where r is the original sample spacing (years/sample) of the ice core ^{10}Be records. This
 19 scaling effectively widens the obtained probability distribution and thus, increases the derived
 20 uncertainties. For the filtered GRIP ^{10}Be record, we assume a decadal resolution.

21 This ‘wobble-matching’ is done for predefined windows of IntCal13 and GRIP and hence,
 22 yields a probability distribution ($P_{s_{scaled}}(t_s)$) for their time scale difference for each window.
 23 We apply this method to 1,000 year windows of $^{14}\text{C}/^{10}\text{Be}$ data and investigate one window
 24 every 50 years back in time. For each window we test for time scale differences (shifts) of \pm
 25 150 years without stretching or compression of the timescale within this window. Hence, in
 26 analogy to ^{14}C -wobble-match dating, each window could be seen as a single 1,000 year long
 27 “tree” that is being calibrated. We tested different window sizes between 500 and 2,000 year
 28 length and the corresponding results are consistent within error. The choice of a 1,000 year
 29 window represents a trade-off between (i) an increasing statistical robustness and hence,

1 smaller uncertainties, and (ii) a loss of detail (variability) in the final transfer function (see
2 also section 2.5) with increasing window length.

3 It can be seen from equation 1, that contrary to the correlation analysis employed by
4 Muscheler et al. (2014a) this method favours $^{10}\text{Be}/^{14}\text{C}$ linkages with a direct 1:1 relationship
5 between IntCal13 and ^{10}Be -based $\Delta^{14}\text{C}$ records. Hence, the $^{14}\text{C}:^{10}\text{Be}$ production rate ratio has
6 to be assessed. Furthermore, the uncertainty for the ^{10}Be -based records and the $^{10}\text{Be}:^{14}\text{C}$
7 conversion is quantitatively included in the calculation and hence, needs to be estimated. In
8 the following sections we will outline how these factors can be initially assessed.

10 **2.3 Assessment of uncertainties due to climatic influences on ^{10}Be**

11 As outlined in the introduction, ice core ^{10}Be records can be affected by various climatic
12 influences that can ‘contaminate’ the production signal. To account for these effects, we use
13 four different versions of the GRIP and GISP2 ^{10}Be records throughout the manuscript. We
14 use ^{10}Be concentrations and fluxes (^{10}Be concentration multiplied by snow accumulation and
15 ice density) as endmembers of the assumed mode of ^{10}Be deposition (wet vs. dry,
16 respectively) on the ice sheet. To address the role of climate influences on ^{10}Be mixing and
17 transport to the ice sheet, we additionally generated “climate corrected” versions of the
18 concentrations and fluxes. For this purpose, we performed multiple linear regression analysis
19 between ^{10}Be and climate proxy time series from the GRIP and GISP2 ice cores. Using ice
20 accumulation rates (Seierstad et al., 2014), $\delta^{18}\text{O}$ (Johnsen et al., 1995; Stuiver et al., 1997),
21 and ion data (Mayewski et al., 1997) as predictors, we linearly detrended the ^{10}Be
22 concentrations and fluxes. This procedure removes covariance between ^{10}Be and climate
23 proxy data and may thus, diminish the climate influences in the ^{10}Be record. It should be
24 noted, that this is a ‘blind’ empirical approach that does not aim for a process based
25 understanding of the climate influences on ^{10}Be . This method would, for example, confound
26 solar (^{10}Be) variations that had an influence on climate as climate influences on ^{10}Be
27 (Adolphi et al., 2014). Hence, these ‘climate corrected’ versions should rather be seen as
28 sensitivity tests for our analysis than as improved estimates of past ^{10}Be production rates per
29 se. In summary, we use four (concentrations, fluxes, and “climate corrected” versions
30 thereof) different versions of the GRIP and GISP2 ^{10}Be data. Each version represents a
31 plausible endmember of the ^{10}Be production rate history, depending on the assumed mode of

1 deposition and climatic impacts on ^{10}Be and can thus, be used to assess the sensitivity of our
2 analysis to these processes.

3

4 **2.4 Assessment of uncertainties due to ^{10}Be – ^{14}C conversion**

5 **2.4.1 Carbon cycle modelling**

6 To be able to compare ^{10}Be to ^{14}C records, we converted the ^{10}Be records into $\Delta^{14}\text{C}$
7 anomalies using a box-diffusion carbon cycle model (Oeschger et al., 1975; Siegenthaler et
8 al., 1980). The model was run under pre-industrial conditions and has been shown to yield
9 consistent results with more complex carbon cycle models for our purposes (Muscheler et al.,
10 2007). As outlined in the introduction, the unknown state and dynamics of the carbon cycle
11 introduce uncertainty to the comparison of ^{10}Be and ^{14}C . To test for the sensitivity to these
12 effects, we conducted four experiments (table 1). Each experiment was forced with an
13 idealized 200 year ^{14}C production rate cycle of $\pm 20\%$ approximately corresponding to a
14 solar de Vries cycle. For two of the experiments we perturbed the state of the carbon cycle by
15 increasing (S1) or decreasing (S2) the air-sea gas exchange constant by 50% mimicking
16 changes in wind speed and/or sea ice extent. In the scenarios S3 and S4 the ocean diffusivity
17 parameter (ocean ventilation) was increased and decreased by 50%, respectively. Each
18 experiment was spun up for 50,000 years under preindustrial conditions until all ^{14}C
19 reservoirs were in steady state. Subsequently the investigated parameter was changed linearly
20 from its preindustrial to its perturbed value within 50 years (transition 1). The perturbed state
21 was then maintained for 25,000 years to reach equilibrium again (steady state) before linearly
22 changing the perturbed parameter back to preindustrial values within 50 years (transition 2).
23 We use these different sensitivity experiments to obtain an uncertainty estimate of the
24 modelled (^{10}Be -based) $\Delta^{14}\text{C}$ records due to carbon cycle effects.

25

26 **2.4.2 $^{10}\text{Be}/^{14}\text{C}$ production rate ratio**

27 To compare tree ring and ice core radionuclide records we used the normalized ^{10}Be records
28 as ^{14}C production rate input for the carbon cycle model. This yields a ^{10}Be -based $\Delta^{14}\text{C}$
29 anomaly record that can be directly compared to the tree-ring data. Hence, we have to assume
30 a ratio between the production rates of ^{14}C and ^{10}Be . This ratio depends on the radionuclide

1 production cross sections and the energy spectrum of the incoming GCR. Model estimates of
2 relative $^{14}\text{C}:$ ^{10}Be production rate increases for a change in the solar modulation parameter
3 from 700 to 0 MeV at modern geomagnetic field strength differ between 1.34 (Masarik and
4 Beer, 2009) and 1.04 (Kovaltsov et al., 2012;Kovaltsov and Usoskin, 2010). Similarly, the
5 predicted $^{14}\text{C}:$ ^{10}Be production rate ratios for changes in the geomagnetic field strength are
6 model dependent for unresolved reasons (Cauquoin, 2014).

7 Furthermore, the $^{14}\text{C}:$ ^{10}Be production rate ratio depends on the presence of a potential ‘polar
8 bias’ (see introduction). If a ‘polar bias’ was present (Bard et al., 1997;Field et al., 2006) the
9 ratio between ^{14}C and ice core ^{10}Be variations could be biased towards lower values. (Bard et
10 al. (1997) report a value of 0.65 for the South Pole ^{10}Be record). For Greenland, however,
11 high resolution ^{10}Be records do not support such a strong polar bias but would instead be
12 consistent with a well mixed atmosphere (Pedro et al., 2012;Muscheler and Heikkilä, 2011).
13 Simply comparing the standard deviations of centennial variations of IntCal13 and ^{10}Be -
14 based $\Delta^{14}\text{C}$ anomalies leads to ratios between 0.95 and 1.05 ($\sigma^{14}\text{C}_{\text{IntCal}}/\sigma^{14}\text{C}_{10\text{Be}}$) depending on
15 which ice core (GRIP/GISP2) and which version of the ^{10}Be records (concentration, flux,
16 climate corrections) is used. Thus, we start with a $^{14}\text{C}:$ ^{10}Be production rate ratio of 1:1 and
17 test the sensitivity of our results to this assumption by repeating the calculations outlined in
18 section 2.2 using $^{14}\text{C}:$ ^{10}Be ratios of 1.5:1 and 0.5:1.

19

20 **2.5 Timescale transfer function**

21 The methodology outlined in section 2.2 yields a probability estimate of the IntCal13-
22 GICC05 timescale difference every 50 years. These probability distributions are however not
23 fully independent since neighbouring 1,000 year windows overlap and are, hence, largely
24 based on the same data. To create a timescale transfer function we employed a Monte-Carlo
25 procedure that creates 20,000 possible transfer functions based on independent, i.e. non-
26 overlapping, windows. Each iteration, i) randomly selects one of the youngest (most recent)
27 20 windows and ii) randomly samples from the probability distribution $P_{\text{scaled}}(t_s)$ of this
28 window as well as the older non-overlapping windows (i.e. one window every 1,000 years so
29 that the selected windows are fully independent with respect to the data points they contain).
30 The resulting transfer functions are then interpolated to annual resolution and converted into
31 probability distributions for the timescale difference at each point in time. For each transfer
32 function we assume that both timescales are correct at 0 BP (i.e. AD 1950).

1

2 **2.6 Iterative structure of the synchronization method**

3 The separate aspects of our synchronization method outlined above are applied in an iterative
4 manner to obtain robust and self consistent error estimates for our results. The different steps
5 involved are carried out in the following order:

- 6 i. We create four versions of both ice core ^{10}Be records as endmembers of plausible
7 ^{10}Be production rate histories (see section 2.3).
- 8 ii. We convert these ^{10}Be records into $\Delta^{14}\text{C}$ using a box-diffusion carbon cycle model
9 (section 2.4.1) assuming a $^{14}\text{C}:^{10}\text{Be}$ production rate ratio of 1 (see section 2.4.2).
- 10 iii. The difference between the different ^{10}Be -based $\Delta^{14}\text{C}$ records, and results from the
11 carbon cycle sensitivity experiments (see section 2.4.1) serve as initial uncertainty
12 estimates for the ^{10}Be -based $\Delta^{14}\text{C}$ records.
- 13 iv. We then compare the tree ring and ^{10}Be -based $\Delta^{14}\text{C}$ records with respect to their
14 timescale differences using the statistics outlined in section 2.2. We test for the
15 robustness of these results by using all four different ^{10}Be versions of GRIP and
16 GISP2 separately as well as ^{10}Be - ^{14}C conversion factors of 0.5 and 1.5 (see section
17 2.4.2).
- 18 v. Calculating an initial timescale transfer function (see section 2.5) we then
19 synchronize IntCal13 and GICC05. This enables us to directly compare tree ring and
20 ^{10}Be -based $\Delta^{14}\text{C}$ records and estimate the optimal $^{14}\text{C}:^{10}\text{Be}$ production rate ratio, as
21 well as uncertainties for the ^{10}Be -based $\Delta^{14}\text{C}$ record.
- 22 vi. Based on these posterior estimates of the $^{14}\text{C}:^{10}\text{Be}$ ratio and the uncertainty of the
23 ^{10}Be records, we repeat the calculations outlined in sections 2.2 and 2.5 yielding our
24 final estimates of the IntCal13-GICC05 timescale differences over the Holocene.

25

26 **3 Results**

27 **3.1 Climate and Carbon cycle related uncertainties in the GRIP and GISP2** 28 **^{10}Be records**

29 Figure 2 displays the different ^{10}Be production rate scenarios from GRIP (top two panels) and
30 GISP2 (lower two panels) ^{10}Be concentrations (Conc), fluxes (Flux) and their climate

1 corrected versions ($\text{Conc}_{\text{clim}}$ and $\text{Flux}_{\text{clim}}$, respectively). Dividing the ^{10}Be records into a
2 centennial (<500 years) and millennial (>500 years) variations indicates that the different
3 ^{10}Be versions mainly differ in the low frequency range. These millennial differences can
4 systematically affect the modelling of $\Delta^{14}\text{C}$ since the carbon cycle acts as an integrator over
5 ^{14}C production rate variations. The centennial changes in the GRIP ^{10}Be versions, however,
6 are highly coherent and indicate a limited climate influence on ^{10}Be on these timescales and
7 the same holds true for the GISP2 ^{10}Be versions. This is in agreement with Adolphi et al.
8 (2014) who showed that centennial GRIP ^{10}Be variations are dominated by solar activity
9 changes and indicate only little sensitivity to the assumed mode of ^{10}Be deposition even over
10 large deglacial climatic transitions. It should be noted that this statement solely refers to the
11 filtered centennial ^{10}Be variations investigated here. Other potential climatic influences on
12 ^{10}Be such as changes in the stratosphere-troposphere exchange rates are, however, difficult to
13 assess from climate proxy data and will thus, not be removed by our detrending technique.
14 Thus, in the following we will focus on centennial (<500 years) changes in ^{10}Be and ^{14}C
15 production rates to avoid systematic errors originating from uncertainties in the millennial
16 ^{10}Be production rate history.

17 The left hand panels in figure 3 show the corresponding modelled $\Delta^{14}\text{C}$ anomalies from the
18 centennial ^{10}Be variations indicated in figure 2 assuming a $^{14}\text{C}:^{10}\text{Be}$ production rate ratio of
19 1:1. As expected, similar to the ^{10}Be records these variations are highly coherent. The right
20 panels in figure 3 display histograms of the maximal $\Delta^{14}\text{C}$ difference between the different
21 production rate histories (i.e. the absolute $\Delta^{14}\text{C}$ difference between the highest and the lowest
22 modelled $\Delta^{14}\text{C}$ version at each point in time). It can be seen that the different ^{10}Be versions
23 translate into a modelled $\Delta^{14}\text{C}$ uncertainty of about $\pm 3 \%$ (1σ) for GRIP (figure 3 a, d) and
24 GISP2 (figure 3 b, e). Similarly, the $\Delta^{14}\text{C}$ anomalies modelled from GRIP and GISP2 ^{10}Be
25 agree within $\pm 2.5 \%$ (1σ , figure 3 c, f).

26 As outlined in the introduction, the state and the dynamics of the carbon cycle impose an
27 uncertainty on the ^{10}Be - ^{14}C comparison that is difficult to quantify from the data itself
28 (Köhler et al., 2006; Muscheler et al., 2004b). Figure 4 shows the results from the performed
29 carbon cycle sensitivity experiments (see section 2.4.1, table 1). It can be seen that the
30 millennial $\Delta^{14}\text{C}$ variations are substantially altered by carbon cycle perturbations (figure 4 b).
31 Changes in ocean ventilation (experiments S3 and S4) and well as air-sea gas exchange
32 (experiments S1 and S2) can cause $\Delta^{14}\text{C}$ anomalies larger than the amplitude of $\Delta^{14}\text{C}$
33 anomalies induced by ^{14}C production rate changes only (control). However, as before, the

1 centennial $\Delta^{14}\text{C}$ variations are considerably less affected by these perturbations (figure 4 c).
2 The increase (decrease) of air-sea gas exchange or ocean ventilation does lead to a decrease
3 (increase) in the amplitude of the modelled centennial $\Delta^{14}\text{C}$ variations. However, these
4 changes in amplitude are largely limited to about $\pm 3 \text{‰}$ (figure 4, panel d) except for about
5 200-300 years around the timing of the carbon cycle perturbation itself (figure 4, transitions 1
6 and 2). Importantly, the phase of the centennial $\Delta^{14}\text{C}$ variations is not affected by the imposed
7 carbon cycle changes. Since the applied carbon cycle changes in our sensitivity experiments
8 are likely unrealistically large for Holocene conditions (Köhler et al., 2006; Roth and Joos,
9 2013), we conservatively assume a 1σ uncertainty of $\pm 3 \text{‰}$ (see figure 4, panel d, ‘steady
10 state’) for the modelled $\Delta^{14}\text{C}$ records due to carbon cycle effects.

11 Adding the uncertainties due to climate impacts on ^{10}Be ($\pm 3 \text{‰}$) and the carbon cycle (± 3
12 ‰) in quadrature we thus, obtain an initial uncertainty estimate of about $\pm 4.5 \text{‰}$ for the
13 modelled $\Delta^{14}\text{C}$ records.

14

15 **3.2 Sensitivity of the synchronization method to uncertainties in the ^{10}Be - ^{14}C** 16 **conversion**

17 In the following we will compare the centennial $\Delta^{14}\text{C}$ (i.e., <500 years, separated by an FFT-
18 based high-pass filter) anomalies reconstructed from tree rings (IntCal13) and ice cores
19 (GRIP/GISP2 ^{10}Be -based) with respect to their timescale differences. The choice of a 500
20 year high-pass filter results from the climate and carbon cycle related uncertainties shown in
21 section 3.1 which increase on longer timescales. We use the statistical framework outlined in
22 section 2.2 and assign an initial uncertainty of $\pm 4.5 \text{‰}$ to the ^{10}Be -based $\Delta^{14}\text{C}$ records. The
23 uncertainties for the tree-ring based $\Delta^{14}\text{C}$ anomalies are taken from IntCal13 (Reimer et al.,
24 2013). For this purpose we spliced the GISP2 ^{10}Be versions into the corresponding GRIP
25 ^{10}Be versions to fill the gap in the GRIP record between 9,400 and 10,800 years BP and
26 create a continuous record for the entire Holocene. Hence, in the following “GRIP” refers to
27 this combination of GRIP and GISP2 data, while results for the GISP2 data are only shown
28 for periods where they have not been used to fill the gap in the GRIP record.

29 Figure 5 displays the obtained probability distributions $P_{\text{scaled}}(t_s)$ for each sliding window,
30 centred on its mean age. The results are shown for all four GRIP ^{10}Be versions (panel a), in
31 comparison to results based on GISP2 data only (panel b), as well as for different assumed

1 $^{14}\text{C}:^{10}\text{Be}$ production rate ratios (panel c). The different GRIP ^{10}Be versions yield consistent
2 estimates of the IntCal13-GICC05 timescale differences throughout the Holocene. The only
3 marked difference occurs around the 8.2 ka BP event (Blockley et al., 2012). During this
4 period the ^{10}Be flux indicates a more rapid increase in the IntCal13-GICC05 timescale
5 difference as compared to all other ^{10}Be versions. As noted by Muscheler et al. (2004a) the
6 accumulation rate anomaly associated to the climate oscillation around 8,200 years ago
7 appears to lead to an ‘over correction’ of the ^{10}Be deposition during flux calculation. This
8 leads to a worse agreement between ^{14}C and ^{10}Be fluxes as compared to ^{14}C and ^{10}Be
9 concentrations (see figure 3 in Muscheler et al., 2004a). This is corroborated by the fact that
10 results based on the “climate corrected” ^{10}Be flux follow the probability estimates of ^{10}Be
11 concentrations (figure 5a).

12 Comparing GRIP based results to GISP2 based estimates indicates consistent estimates of the
13 timescale differences. The larger uncertainties of the GISP2 based results are due to the lower
14 sampling resolution of the GISP2 ^{10}Be record (see equation 3).

15 Figure 5c shows the sensitivity of our results to the assumed $^{14}\text{C}:^{10}\text{Be}$ production rate ratio. It
16 can be seen that the inferred timescale differences are relatively insensitive to the assumed
17 $^{14}\text{C}:^{10}\text{Be}$ ratio. However, the derived uncertainty of $P_{scaled}(t_s)$ does increase with lower
18 $^{14}\text{C}:^{10}\text{Be}$ ratios. This can easily be understood by imagining a scaling of zero for the ^{10}Be -
19 based record which would result in an infinitely wide probability distribution.

20 In summary, our method of estimating the IntCal13-GICC05 timescale difference is i) largely
21 robust for all versions of the GRIP ^{10}Be record, ii) consistent for GRIP and GISP2 ^{10}Be data,
22 and iii) independent of the assumed $^{14}\text{C}:^{10}\text{Be}$ production rate ratio. However, this analysis
23 also shows that it is important to compare ^{10}Be concentrations and fluxes to identify potential
24 caveats as seen around the 8.2 ka BP event. Furthermore, while the estimate of the most
25 likely timescale difference (i.e. the location of the maximum of $P_{scaled}(t_s)$) may not be
26 affected by the assumed $^{14}\text{C}:^{10}\text{Be}$ ratio, the uncertainty of this estimate is. Hence, in the
27 following section we will derive a posterior estimate of the $^{14}\text{C}:^{10}\text{Be}$ ratio, as well as a refined
28 uncertainty estimate of the ^{10}Be -based $\Delta^{14}\text{C}$ records.

29

3.3 Posterior estimate of the $^{14}\text{C}:^{10}\text{Be}$ production rate ratios and uncertainties

As shown in the previous section, our estimates of the most likely timescale difference between IntCal13 and GICC05 are largely independent of which ^{10}Be record (GRIP/GISP2) and which version thereof (concentration, flux, climate corrections) is used, as well as which $^{14}\text{C}:^{10}\text{Be}$ ratio is assumed. Hence, we calculated an initial GICC05-IntCal13 transfer function (section 2.5) and synchronized the tree ring based and ^{10}Be -based $\Delta^{14}\text{C}$ record. This enables us to compare the records with respect to the most likely $^{14}\text{C}:^{10}\text{Be}$ ratio. In addition, we can derive a posterior estimate of the modelled ^{10}Be -based $\Delta^{14}\text{C}$ uncertainty.

After synchronization we can compare tree ring and ^{10}Be -based $\Delta^{14}\text{C}$ sample pairs assuming different ^{10}Be scaling factors (i.e. $^{14}\text{C}:^{10}\text{Be}$ ratios) between zero and two. The difference between tree ring and ^{10}Be -based $\Delta^{14}\text{C}$ sample pairs ($\delta(t)$) is a function of the uncertainty of IntCal13 ($\delta_{IC}(t)$) and the uncertainty of the ^{10}Be -based records ($\delta_{Be}(t)$) in the form that:

$$\delta(t) = \sqrt{\delta(t)_{IC}^2 + \delta(t)_{Be}^2} \quad (4)$$

Hence, we can rearrange equation 4 and use the quoted uncertainties of IntCal13 to derive $\delta(t)_{Be}$:

$$\delta(t)_{Be} = \sqrt{\delta(t)^2 - \delta(t)_{IC}^2}; \quad \delta(t) > \delta(t)_{IC} \quad (5)$$

$$\delta(t)_{Be} = 0; \quad \delta(t) \leq \delta(t)_{IC}$$

These uncertainties can be summarized to the rooted mean square error ($\text{RMSE}_{10\text{Be}}$). This way we can obtain the optimal ^{10}Be scaling factor (where the $\text{RMSE}_{10\text{Be}}$ minimizes) and the associated uncertainty of the ^{10}Be -based $\Delta^{14}\text{C}$ records (the minimum of the $\text{RMSE}_{10\text{Be}}$). Figure 6 displays the results of this analysis indicating an optimal ^{10}Be scaling factor of around 0.7. Assuming that the centennial ^{10}Be and ^{14}C production rate changes are mainly modulated through solar activity this low scaling factor would point to a strong polar bias of the GRIP GISP2 ^{10}Be records (see sections 1 and 2.4.2). However, when investigating the $\Delta^{14}\text{C}$ time series it becomes apparent, that this low scaling leads to an underestimation of the amplitude of virtually all grand solar maxima and minima (i.e. large $\Delta^{14}\text{C}$ anomalies) in the ^{10}Be -based $\Delta^{14}\text{C}$ record (figure 7, top). This bias is induced by the fact, that the $\Delta^{14}\text{C}$ anomalies are normally distributed around 0 ‰ leading to a majority of the $\Delta^{14}\text{C}$ values lying close to zero dominating the $\text{RMSE}_{10\text{Be}}$. Hence, for these values a low scaling of the ^{10}Be -based $\Delta^{14}\text{C}$ records will simply act to reduce noise from the record and thus, reduce the $\text{RMSE}_{10\text{Be}}$.

1 To avoid this bias, we performed a binned regression analysis. We divided the tree ring and
2 ^{10}Be -based $\Delta^{14}\text{C}$ sample pairs into bins of 2.5 ‰ (defined based on the tree ring $\Delta^{14}\text{C}$
3 anomalies) and calculated the $\text{RMSE}_{10\text{Be}}$ for each bin ($\text{RMSE}_{10\text{Be}_{\text{bin}}}$). These uncertainties for
4 each bin can then be summarized to an overall $\text{RMSE}_{10\text{Be}}$ as:

$$5 \quad \text{RMSE}_{10\text{Be}} = \sqrt{\text{RMSE}_{10\text{Be}_{\text{bin}}}^2} \quad (6)$$

6 This binning leads to an equal weighting of small and large $\Delta^{14}\text{C}$ anomalies in the
7 comparison of the $\Delta^{14}\text{C}$ records. It can be seen that this method indicates a larger $^{14}\text{C}:^{10}\text{Be}$
8 ratio of about 1.1 (figure 8) and avoids the systematic underestimation of large amplitude
9 $\Delta^{14}\text{C}$ anomalies (figure 7, bottom). Depending on the production rate model used, this scaling
10 indicates a weak (Masarik and Beer, 2009, 1999) or no (Kovaltsov et al., 2012; Kovaltsov and
11 Usoskin, 2010) polar bias in the Greenland ^{10}Be records. In addition, it can be seen that the
12 minimum of the $\text{RMSE}_{10\text{Be}}$ becomes larger than without binning, indicating an uncertainty of
13 about 4 ‰ for the ^{10}Be -based $\Delta^{14}\text{C}$ records. This is due to the above described effect, that the
14 noise is not artificially suppressed and can be seen by comparing the decadal scale peaks in the
15 top and bottom panels of figure 7. The larger ^{10}Be scaling factor makes the ^{10}Be record
16 appear noisier. However, firstly, this noise may represent remaining influences of ‘system
17 effects’ on ice core ^{10}Be records and hence, represent an uncertainty that has to be taken into
18 account. Secondly, it should be kept in mind that IntCal13 is a stack of multiple ^{14}C datasets
19 which will inevitably result in smoothing. This smoothing may also reduce the amplitude of
20 ‘real’ $\Delta^{14}\text{C}$ variations instead of merely reducing noise, since the differences between the
21 underlying raw data sets of IntCal13 are potentially in part systematic (Stuiver et al.,
22 1998; Adolphi et al., 2013).

23 In conclusion we use a $^{14}\text{C}:^{10}\text{Be}$ ratio of 1.1:1 and an uncertainty of 4 ‰ for the modelled
24 $\Delta^{14}\text{C}$ record to derive a final IntCal13-GICC05 transfer function in the next section. **It should
25 be noted that this uncertainty estimate is only valid for the centennial (<500 year) variations
26 studied here.**

27

28 **3.4 IntCal13-GICC05 transfer function**

29 Using the estimated $^{14}\text{C}:^{10}\text{Be}$ ratio of 1.1 and a ^{10}Be -based $\Delta^{14}\text{C}$ error of ± 4 ‰ ($\pm 1\sigma$) (see
30 previous section) we recalculated the ‘wobble-match’ probability distributions ($P_{\text{scaled}}(t_s)$,

1 equation 3) for the IntCal13-GICC05 timescale difference (figure 9, grey shading). For these
2 calculations we used the mean of all GRIP¹⁰Be-based $\Delta^{14}\text{C}$ versions (concentration, flux,
3 climate corrections) and filled the gap between 9,400 and 10,800 yrBP using the GISP2 data.
4 Based on these probability distributions we modelled the IntCal13-GICC05 transfer function
5 as described in section 2.5. The resulting transfer function (figure 9 solid lines) averages out
6 some short-term fluctuations in the timescale difference compared to the initial ‘wiggles-
7 match’ probability distributions. As described in section 2.5 this is due to the used window
8 length of 1,000 years to determine $P_{scaled}(t_s)$ at each point in time, preventing an
9 independent assessment of faster changes in the timescale difference. Nevertheless, the
10 estimated uncertainties of the timescale transfer function (thin black lines in figure 9)
11 encompass the uncertainties of the ‘wiggles-match’ probability distribution at each point in
12 time.

13 Figure 10 shows three examples of GRIP ¹⁰Be based $\Delta^{14}\text{C}$ anomalies before (grey) and after
14 (black) synchronization to IntCal13 (red). The examples encompass (i) a period of relatively
15 low $\Delta^{14}\text{C}$ variability ($\pm 5\text{-}7\%$) but good agreement between GRIP and IntCal13 (figure 10, a),
16 (ii) a period of large $\Delta^{14}\text{C}$ variability ($\pm 10\%$) but less good agreement between GRIP and
17 IntCal13 (figure 10, b), and (iii) a section of large $\Delta^{14}\text{C}$ ($\pm 10\%$) variability and excellent
18 agreement between GRIP and IntCal13 (figure 10, c). It can be seen, that in all cases the fit
19 between GRIP and IntCal13 is improved when applying the proposed GICC05-IntCal13
20 transfer function. However, figure 10 (b) also shows, that short periods of disagreement (i.e.,
21 around 7,250 – 7,500 years BP) may remain, as they cannot be reliably resolved by our
22 method which matches 1,000 year-long sections. It should, however, be noted that matching
23 these short sections would (i) represent a serious violation of the GICC05 counting error
24 which is minimal over these short periods of time (± 6 years at 2σ between 7,250 – 7,500
25 years BP), and (ii) not account for the possibility that ¹⁰Be and ¹⁴C may simply not agree due
26 to the caveats outlined in the introduction. Furthermore, the applied shift of GICC05 in figure
27 10 (b) leads to an improved agreement between ¹⁴C and ¹⁰Be after and prior to 7,250 and
28 7,500, respectively. Hence, we consider it unlikely that for this short period of time the
29 timescale difference deviates significantly from the estimate for the entire window.

30

1 4 Discussion

2 Figure 11 shows the obtained estimate of the IntCal13-GICC05 timescale difference in
3 comparison to the results obtained by using the method of Muscheler et al. (2014a, re-run
4 with a 1,000 year window length) and age markers that have been independently anchored on
5 both timescales.

6 Our results are fully consistent with the results obtained by Muscheler et al. (2014a). While
7 this is expected to some extent, as our study and the work by Muscheler et al. (2014a) are
8 based on the same data, it shows that the statistical approach used here leads to similar results
9 as the Monte-Carlo lag-correlation analysis but is computationally much less expensive.
10 Furthermore, as shown in figure 5, we obtain similar results when using the GISP2 ^{10}Be
11 instead of the GRIP ^{10}Be record lending additional support to the robustness of our results.
12 The additional modelling of the transfer function employed here (sections 2.5 and 3.4) leads
13 to a smoother development of the timescale difference which is more realistically reflecting
14 limitations of the method imposed by the window size of the ^{14}C - ^{10}Be comparison. The
15 difference between the timescale transfer functions around 8,200 years BP is induced by the
16 fact that Muscheler et al. (2014a) based their calculations on ^{10}Be fluxes which are influenced
17 by accumulation rate changes around this time as discussed in section 3.2 and in Muscheler et
18 al. (2004a).

19 The largest difference between the results presented here and by those of Muscheler et al.
20 (2014a) is seen in the derived error estimates. We obtain strongly reduced uncertainties for
21 the estimated timescale differences. This is likely due to the fact, that Muscheler et al.
22 (2014a) used a comparably ad-hoc and highly conservative method to derive their
23 uncertainties. By taking the distribution of the mean r^2 -values of all iterations Muscheler et al.
24 (2014a) do not include the results of the Monte-Carlo analysis of the “Best Fits” in their error
25 estimate. Thus, ^{14}C - ^{10}Be matches that may not be the most likely solution in any of the
26 iterations become included in the uncertainty envelope. In comparison, the statistics
27 employed here allow a direct analytical assessment of the synchronization uncertainties.
28 Hence, while our uncertainty estimates are significantly smaller, we consider them more
29 robust. Theoretically, systematic errors from undetected biases in the ^{10}Be record could lead
30 to erroneous results. However, the results shown in section 3.2 demonstrate the consistency
31 of GRIP and GISP2 ^{10}Be -based calculations as well as for different climate corrections and
32 do, thus, not indicate such biases (see figure 5). In conclusion, while largely consistent, we

1 regard the method employed here a significant improvement to the approach by Muscheler et
2 al. (2014a).

3 Comparing our results to independent estimates of IntCal13-GICC05 timescale differences
4 further supports our analyses (figure 11, symbols). Two major solar proton events (“775 and
5 994 AD events”) leaving well defined spikes in the ^{14}C content of dendrochronologically
6 dated trees (Miyake et al., 2013;Miyake et al., 2012;Güttler et al., 2015) as well as in
7 Greenland ice core ^{10}Be records (Mekhaldi et al., 2015;Sigl et al., 2015) indicate an IntCal13-
8 GICC05 timescale difference of -7 ± 2 (2σ) years for both events (Sigl et al., 2015).
9 Consistent with these findings, we obtain IntCal13-GICC05 differences of -4 ± 4 and -6 ± 5
10 years (2σ) for the 994 and 775 AD event, respectively. It should be noted that these annual
11 radionuclide excursions are not present in the data used here, which is of lower resolution,
12 and are hence, independent estimates of the timescale difference.

13 Based on tephra findings in the GRIP ice core (Barbante et al., 2013) the historically dated
14 AD 79 eruption of Vesuvius has been used as a reference point in the GICC05 chronology
15 (Vinther et al., 2006). However, our results indicate a timescale offset of -11 ± 6 (2σ) years at
16 AD 79 (1871 years BP, see figure 11). Assuming that the tree-ring chronologies are correct at
17 this time, this would imply an age of $\text{AD } 90 \pm 6$ for the GRIP tephra layer – incompatible
18 with an attribution to the age of the Vesuvius eruption within 2σ . This result is in agreement
19 with the analysis by Sigl et al. (2015) who recently counted annual layers in the NEEM and
20 NEEM-2011-S1 ice cores and dated this marker horizon to AD 87 and 89, respectively.

21 The age of the Minoan eruption of Santorini has long been debated and the presence of an
22 unequivocally attributable signal in the ice core records has been questioned (Pearce et al.,
23 2004;Hammer et al., 1987;Hammer et al., 2003;Friedrich et al., 2006). The GICC05 age of
24 3591 ± 5 BP of an identified tephra horizon is incompatible with the radiocarbon based age of
25 3563 ± 14 calBP of the Santorini eruption ($\Delta = -28 \pm 15$ yrs). Our results indicate a
26 chronology difference of -20 ± 5 years around this time, reconciling the two aforementioned
27 ages (see figure 11, open diamond). Hence, at least from a chronological point of view, it
28 cannot be ruled out that the ice core tephra may be ascribable to the Santorini eruption
29 (Muscheler, 2009).

30 Volcanic glass shards from the Saksunarvatn ash have been found in the GRIP ice core
31 (Grönvold et al., 1995), as well as in multiple marine, lacustrine and terrestrial sites, of which
32 the Lake Kråkenes record provides the highest resolution radiocarbon based age for the

1 deposit (Lohne et al., 2013). The dating difference of -86 ± 35 years between the radiocarbon
2 based age by Lohne et al. ($10,210 \pm 35$ calBP, $\pm 1\sigma$) and the GICC05 age (10,296 BP, Abbott
3 and Davies, 2012) of the Saksunarvatn ash is consistent with our estimated timescale
4 difference of -66 ± 10 years during this time interval.

5 In summary, our results are consistent within uncertainties with all independent age markers
6 that link the GICC05 and IntCal13 timescales over the Holocene.

7 Figure 12 displays the inferred IntCal13-GICC05 timescale differences in comparison to the
8 GICC05 maximum counting error (Rasmussen et al., 2006; Vinther et al., 2006). Assuming
9 that the tree-ring chronologies underlying IntCal13 are accurate throughout the Holocene our
10 results imply an underestimation of the absolute dating uncertainty of GICC05 for large parts
11 of the Holocene. Furthermore, it can be seen that the counting error appears to be systematic,
12 in that most uncertain years (counted as 0.5 ± 0.5 years, Rasmussen et al., 2006) have indeed
13 not been true calendar years during the Holocene (i.e., a systematic over-counting of years).
14 Nevertheless, when comparing the rate of change of the inferred IntCal13-GICC05 timescale
15 difference to the rate of change of the maximum counting error (i.e. the relative maximum
16 counting error) it can be seen that – even though systematic – the identification of uncertain
17 years in the ice core records is accurate. Except for the most recent 2,000 years where
18 (potentially erroneous) fix-points like the Vesuvius eruption are used to constrain GICC05
19 the relative layer counting uncertainty appears to be an accurate uncertainty estimate. This
20 can be seen in figure 12 (lower panel) which indicates that the rate of change of the GICC05
21 maximum counting error is consistent within error with the rate of change of the IntCal13-
22 GICC05 timescale difference prior to 2,000 years BP. This is important to note as it generally
23 supports the GICC05 layer counting methodology and uncertainty which forms the basis of
24 GICC05 back to 60,000 years BP (Svensson et al., 2008), even though the systematic nature
25 of the derived timescale differences challenges the use of the maximum counting error as a
26 nearly Gaussian distributed 2σ uncertainty during the Holocene (Andersen et al., 2006). It
27 can, however, not be assumed that the counting error continues to be systematic beyond this
28 period, since the parameters used for layer identification as well as the sources of uncertainty
29 (e.g. melt layers) differ back in time under changed climatic conditions (Rasmussen et al.,
30 2006).

31 Alternatively, uncertainties in the dendrochronologies underlying IntCal13 could contribute
32 to the growing discrepancy between IntCal13 and GICC05 over the Holocene. This appears,
33 however, unlikely since the tree-ring chronologies have been cross-dated back to 7,272 calBP

1 to the Irish Oak Chronology (Pilcher et al., 1984) and back to 9,741 calBP using
2 independently constructed German Oak Chronologies (Friedrich et al., 2004; Spurk et al.,
3 2002). Furthermore, the gradual development of the timescale difference appears consistent
4 with a counting uncertainty, while a dendrochronological mismatch could be expected to
5 cause sudden ‘jumps’ in the timescale difference. However, consistently missing tree rings in
6 both German oak chronologies for the period older than 7,272 calBP could theoretically
7 contribute to the growing timescale difference.

8

9 **5 Conclusions**

10 We employed a novel approach to infer timescale differences between two of the most widely
11 used chronologies in Holocene paleoclimatology, the radiocarbon (IntCal13, Reimer et al.,
12 2013) and Greenland ice core (GICC05, Svensson et al., 2008) timescales. Our results are
13 largely consistent with the results of Muscheler et al. (2014a) but yield significantly smaller
14 and more robust uncertainty estimates. The inferred timescale differences are consistent with
15 independent tie-points obtained from volcanic tephtras and solar proton events. However, in
16 agreement with Sigl et al. (2015) our analyses indicate that the attribution of an ice core
17 tephtra to the AD 79 eruption of Vesuvius (Barbante et al., 2013) may be erroneous which
18 leads to a propagating ice core dating bias that affects large parts of the Holocene.
19 Nevertheless, the identification of uncertain years in the ice core during the Holocene is
20 otherwise generally accurate as expressed in the relative counting error (figure 12 lower
21 panel). This is important to note as it, in principle, supports the layer counting method and
22 uncertainty estimates also beyond the period investigated here. Furthermore, it should be
23 noted that these conclusions are based on the assumption that the tree-ring time scale is
24 accurate.

25 Independent of the accuracy of either of the two chronologies we provided a high precision
26 transfer function between the radiocarbon and Greenland ice core timescales. This allows
27 radiocarbon dated and ice core paleoclimate records to be compared at high chronological
28 precision which will improve studies of leads and lags within the climate system throughout
29 the Holocene (Bronk Ramsey et al., 2014). Furthermore, the methodology outlined here can
30 be applied to link high resolution ^{14}C records such as floating tree-ring chronologies to ice
31 core time scales and thus, aid in testing and improving the glacial radiocarbon dating
32 calibration curve.

1 The proposed GICC05-IntCal13 transfer function shown in figure 9, 11 and 12 is available as
2 a supplementary file to this paper and on NOAA.

4 Acknowledgements

5 The study was supported by the Swedish Research Council (VR) through a Linnaeus grant to
6 Lund University (LUCCI). This work was supported by a grant from the Swedish Research
7 Council (Dnr: 2013-8421). We thank Anders Svensson for providing GICC05 snow
8 accumulation rates.

10 References

- 11 Abbott, P. M., and Davies, S. M.: Volcanism and the Greenland ice-cores: the tephra record,
12 Earth-Science Reviews, 115, 173-191,
13 <http://dx.doi.org/10.1016/j.earscirev.2012.09.001>, 2012.
- 14 Adolphi, F., Güttler, D., Wacker, L., Skog, G., and Muscheler, R.: Intercomparison of 14C
15 dating of wood samples at Lund University and ETH-Zurich AMS facilities: extraction,
16 graphitization, and measurement, Radiocarbon, 55, 391-400, 2013.
- 17 Adolphi, F., Muscheler, R., Svensson, A., Aldahan, A., Possnert, G., Beer, J., Sjolte, J., Björck,
18 S., Matthes, K., and Thiéblemont, R.: Persistent link between solar activity and
19 Greenland climate during the Last Glacial Maximum, Nat Geosci, 7, 662-666,
20 10.1038/ngeo2225, 2014.
- 21 Alley, R. B., Finkel, R. C., Nishiizumi, K., Anandakrishnan, S., Shuman, C. A., Mershon, G.,
22 Zielinski, G. A., and Mayewski, P. A.: Changes in Continental and Sea-Salt
23 Atmospheric Loadings in Central Greenland during the Most Recent Deglaciation -
24 Model-Based Estimates, Journal of Glaciology, 41, 503-514, 1995.
- 25 Andersen, K. K., Svensson, A., Johnsen, S. J., Rasmussen, S. O., Bigler, M., Röthlisberger, R.,
26 Ruth, U., Siggaard-Andersen, M.-L., Peder Steffensen, J., and Dahl-Jensen, D.: The
27 Greenland Ice Core Chronology 2005, 15–42ka. Part 1: constructing the time scale,
28 Quaternary Sci Rev, 25, 3246-3257, 10.1016/j.quascirev.2006.08.002, 2006.
- 29 Barbante, C., Kehrwald, N. M., Marianelli, P., Vinther, B. M., Steffensen, J. P., Cozzi, G.,
30 Hammer, C. U., Clausen, H. B., and Siggaard-Andersen, M. L.: Greenland ice core
31 evidence of the 79 AD Vesuvius eruption, Clim. Past, 9, 1221-1232, 10.5194/cp-9-
32 1221-2013, 2013.
- 33 Bard, E., Raisbeck, G. M., Yiou, F., and Jouzel, J.: Solar modulation of cosmogenic nuclide
34 production over the last millennium: comparison between 14C and 10Be records,
35 Earth Planet Sc Lett, 150, 453-462, 10.1016/S0012-821X(97)00082-4, 1997.
- 36 Blockley, S. P. E., Lane, C. S., Hardiman, M., Rasmussen, S. O., Seierstad, I. K., Steffensen, J.
37 P., Svensson, A., Lotter, A. F., Turney, C. S. M., and Bronk Ramsey, C.:
38 Synchronisation of palaeoenvironmental records over the last 60,000 years, and an
39 extended INTIMATE event stratigraphy to 48,000 b2k, Quaternary Sci Rev, 36, 2-10,
40 10.1016/j.quascirev.2011.09.017, 2012.

- 1 Blunier, T., Chappellaz, J., Schwander, J., Dällenbach, A., Stauffer, B., Stocker, T. F., Raynaud,
2 D., Jouzel, J., Clausen, H. B., Hammer, C. U., and Johnsen, S. J.: Asynchrony of
3 Antarctic and Greenland climate change during the last glacial period, *Nature*, 394,
4 739-743, 10.1038/29447, 1998.
- 5 Bronk Ramsey, C., van der Plicht, J., and Weninger, B.: " Wiggle matching" radiocarbon
6 dates, *Radiocarbon*, 43, 381-390, 2001.
- 7 Bronk Ramsey, C., Albert, P., Blockley, S., Hardiman, M., Lane, C., Macleod, A., Matthews, I.
8 P., Muscheler, R., Palmer, A., and Staff, R. A.: Integrating timescales with time-
9 transfer functions: a practical approach for an INTIMATE database, *Quaternary Sci*
10 *Rev*, 106, 67-80, 10.1016/j.quascirev.2014.05.028, 2014.
- 11 Buizert, C., Adrian, B., Ahn, J., Albert, M., Alley, R. B., Baggenstos, D., Bauska, T. K., Bay, R. C.,
12 Bencivengo, B. B., Bentley, C. R., Brook, E. J., Chellman, N. J., Clow, G. D., Cole-Dai, J.,
13 Conway, H., Cravens, E., Cuffey, K. M., Dunbar, N. W., Edwards, J. S., Fegyveresi, J.
14 M., Ferris, D. G., Fitzpatrick, J. J., Fudge, T. J., Gibson, C. J., Gkinis, V., Goetz, J. J.,
15 Gregory, S., Hargreaves, G. M., Iverson, N., Johnson, J. A., Jones, T. R., Kalk, M. L.,
16 Kippenhan, M. J., Koffman, B. G., Kreutz, K., Kuhl, T. W., Lebar, D. A., Lee, J. E.,
17 Marcott, S. A., Markle, B. R., Maselli, O. J., McConnell, J. R., McGwire, K. C., Mitchell,
18 L. E., Mortensen, N. B., Neff, P. D., Nishiizumi, K., Nunn, R. M., Orsi, A. J., Pasteris, D.
19 R., Pedro, J. B., Pettit, E. C., Price, P. B., Priscu, J. C., Rhodes, R. H., Rosen, J. L.,
20 Schauer, A. J., Schoenemann, S. W., Sendelbach, P. J., Severinghaus, J. P.,
21 Shturmakov, A. J., Sigl, M., Slawny, K. R., Souney, J. M., Sowers, T. A., Spencer, M. K.,
22 Steig, E. J., Taylor, K. C., Twickler, M. S., Vaughn, B. H., Voigt, D. E., Waddington, E. D.,
23 Welten, K. C., Wendricks, A. W., White, J. W. C., Winstrup, M., Wong, G. J., and
24 Woodruff, T. E.: Precise inter-polar phasing of abrupt climate change during the last
25 ice age, *Nature*, 520, 661-665, 10.1038/nature14401
- 26 [http://www.nature.com/nature/journal/v520/n7549/abs/nature14401.html#supplementar](http://www.nature.com/nature/journal/v520/n7549/abs/nature14401.html#supplementary-information)
27 [y-information](http://www.nature.com/nature/journal/v520/n7549/abs/nature14401.html#supplementary-information), 2015.
- 28 Cauquoin, A.: Use of ^{10}Be to Predict Atmospheric ^{14}C Variations during the Laschamp
29 Excursion: High Sensitivity to Cosmogenic Isotope Production Calculations,
30 *Radiocarbon*, 56, 67-82, 10.2458/56.16478, 2014.
- 31 Delaygue, G., and Bard, E.: An Antarctic view of Beryllium-10 and solar activity for the past
32 millennium, *Clim Dynam*, 36, 2201-2218, 10.1007/s00382-010-0795-1, 2010.
- 33 Elsässer, C., Wagenbach, D., Levin, I., Stanzick, A., Christl, M., Wallner, A., Kipfstuhl, S.,
34 Seierstad, I. K., Wershofen, H., and Dibb, J.: Simulating ice core ^{10}Be on the glacial-
35 interglacial timescale, *Clim. Past*, 11, 115-133, 10.5194/cp-11-115-2015, 2015.
- 36 Field, C. V., Schmidt, G. A., Koch, D., and Salyk, C.: Modeling production and climate-related
37 impacts on ^{10}Be concentration in ice cores, *J Geophys Res*, 111, D15107,
38 10.1029/2005jd006410, 2006.
- 39 Finkel, R. C., and Nishiizumi, K.: Beryllium 10 concentrations in the Greenland Ice Sheet
40 Project 2 ice core from 3–40 ka, *J Geophys Res*, 102, 26699, 10.1029/97jc01282,
41 1997.
- 42 Friedrich, M., Remmele, S., Kromer, B., Hofmann, J., Spurk, M., Kaiser, K. F., Orsel, C., and
43 Küppers, M.: The 12,460-year Hohenheim oak and pine tree-ring chronology from

- 1 central Europe—a unique annual record for radiocarbon calibration and
2 paleoenvironment reconstructions, *Radiocarbon*, 46, 1111-1122, 2004.
- 3 Friedrich, W. L., Kromer, B., Friedrich, M., Heinemeier, J., Pfeiffer, T., and Talamo, S.:
4 Santorini Eruption Radiocarbon Dated to 1627-1600 B.C, *Science*, 312, 548,
5 10.1126/science.1125087, 2006.
- 6 Grönvold, K., Óskarsson, N., Johnsen, S. J., Clausen, H. B., Hammer, C. U., Bond, G., and Bard,
7 E.: Ash layers from Iceland in the Greenland GRIP ice core correlated with oceanic
8 and land sediments, *Eart Planet Sc Lett*, 135, 149-155,
9 [http://dx.doi.org/10.1016/0012-821X\(95\)00145-3](http://dx.doi.org/10.1016/0012-821X(95)00145-3), 1995.
- 10 Güttler, D., Adolphi, F., Beer, J., Bleicher, N., Boswijk, G., Christl, M., Hogg, A., Palmer, J.,
11 Vockenhuber, C., Wacker, L., and Wunder, J.: Rapid increase in cosmogenic ¹⁴C in AD
12 775 measured in New Zealand kauri trees indicates short-lived increase in ¹⁴C
13 production spanning both hemispheres, *Eart Planet Sc Lett*, 411, 290-297,
14 10.1016/j.epsl.2014.11.048, 2015.
- 15 Hammer, C. U., Clausen, H. B., Friedrich, W. L., and Tauber, H.: The Minoan eruption of
16 Santorini in Greece dated to 1645 BC?, *Nature*, 328, 517-519, 1987.
- 17 Hammer, C. U., Kurat, G., Hoppe, P., Grum, W., and Clausen, H. B.: Thera eruption date 1645
18 BC confirmed by new ice core data?, *Proceedings of the SCIEM 2000 -*
19 *EuroConference Haindorf*, May 2001, Haindorf, 2003, 87-93,
- 20 Heikkilä, U., Beer, J., and Feichter, J.: Meridional transport and deposition of atmospheric
21 ¹⁰Be, *Atmospheric Chemistry and Physics*, 9, 515-527, 10.5194/acp-9-515-2009,
22 2009.
- 23 Heikkilä, U., Beer, J., Abreu, J. A., and Steinhilber, F.: On the Atmospheric Transport and
24 Deposition of the Cosmogenic Radionuclides (¹⁰Be): A Review, *Space Science*
25 *Reviews*, 176, 321-332, 10.1007/s11214-011-9838-0, 2011.
- 26 Heikkilä, U., and Smith, A. M.: Production rate and climate influences on the variability
27 of ¹⁰Be deposition simulated by ECHAM5-HAM: Globally, in Greenland, and in
28 Antarctica, *J Geophys Res-Atmos*, 118, 2506-2520, 10.1002/jgrd.50217, 2013.
- 29 Hogg, A. G., Turney, C. S., Palmer, J. G., Southon, J., Kromer, B., Ramsey, C. B., Boswijk, G.,
30 Fenwick, P., Noronha, A., and Staff, R.: The New Zealand kauri (*Agathis australis*)
31 research project: a radiocarbon dating intercomparison of Younger Dryas wood and
32 implications for IntCal13, *Radiocarbon*, 55, 2035-2048, 2013.
- 33 Johnsen, S. J., Dahl-Jensen, D., Dansgaard, W., and Gundestrup, N.: Greenland
34 palaeotemperatures derived from GRIP bore hole temperature and ice core isotope
35 profiles, *Tellus B*, 47, 624-629, 10.1034/j.1600-0889.47.issue5.9.x, 1995.
- 36 Köhler, P., Muscheler, R., and Fischer, H.: A model-based interpretation of low-frequency
37 changes in the carbon cycle during the last 120,000 years and its implications for the
38 reconstruction of atmospheric $\Delta^{14}\text{C}$, *Geochemistry, Geophysics, Geosystems*, 7,
39 Q11N06, 10.1029/2005GC001228, 2006.
- 40 Kovaltsov, G. A., and Usoskin, I. G.: A new 3D numerical model of cosmogenic nuclide ¹⁰Be
41 production in the atmosphere, *Eart Planet Sc Lett*, 291, 182-188,
42 10.1016/j.epsl.2010.01.011, 2010.

- 1 Kovaltsov, G. A., Mishev, A., and Usoskin, I. G.: A new model of cosmogenic production of
2 radiocarbon ^{14}C in the atmosphere, *Eart Planet Sc Lett*, 337-338, 114-120,
3 10.1016/j.epsl.2012.05.036, 2012.
- 4 Lal, D., and Peters, B.: Cosmic ray produced radioactivity on the earth, in: *Kosmische*
5 *Strahlung II/Cosmic Rays II*, Springer, 551-612, 1967.
- 6 Lane, C. S., Brauer, A., Blockley, S. P. E., and Dulski, P.: Volcanic ash reveals time-
7 transgressive abrupt climate change during the Younger Dryas, *Geology*, 41, 1251-
8 1254, 10.1130/g34867.1, 2013.
- 9 Lohne, Ø. S., Mangerud, J. A. N., and Birks, H. H.: Precise ^{14}C ages of the Vedde and
10 Saksunarvatn ashes and the Younger Dryas boundaries from western Norway and
11 their comparison with the Greenland Ice Core (GICC05) chronology, *Journal of*
12 *Quaternary Science*, 28, 490-500, 10.1002/jqs.2640, 2013.
- 13 Masarik, J., and Beer, J.: Simulation of particle fluxes and cosmogenic nuclide production in
14 the Earth's atmosphere, *J Geophys Res-Atmos*, 104, 12099-12111, Doi
15 10.1029/1998jd200091, 1999.
- 16 Masarik, J., and Beer, J.: An updated simulation of particle fluxes and cosmogenic nuclide
17 production in the Earth's atmosphere, *J Geophys Res*, 114, D11103,
18 10.1029/2008jd010557, 2009.
- 19 Mayewski, P. A., Meeker, L. D., Twickler, M. S., Whitlow, S., Yang, Q., Lyons, W. B., and
20 Prentice, M.: Major features and forcing of high-latitude northern hemisphere
21 atmospheric circulation using a 110,000-year-long glaciochemical series, *J Geophys*
22 *Res*, 102, 26345, 10.1029/96jc03365, 1997.
- 23 Mekhaldi, F., Muscheler, R., Adolphi, F., Aldahan, A., Beer, J., McConnell, J. R., Possnert, G.,
24 Sigl, M., Svensson, A., Synal, H.-A., Welten, K. C., and Woodruff, T. E.:
25 Multiradionuclide evidence for the solar origin of the cosmic-ray events of AD 774/5
26 and 993/4, *Nat Commun*, 6, 10.1038/ncomms9611, 2015.
- 27 Miyake, F., Nagaya, K., Masuda, K., and Nakamura, T.: A signature of cosmic-ray increase in
28 AD 774-775 from tree rings in Japan, *Nature*, 486, 240-242, 10.1038/nature11123,
29 2012.
- 30 Miyake, F., Masuda, K., and Nakamura, T.: Another rapid event in the carbon-14 content of
31 tree rings, *Nat Commun*, 4, 1748, 10.1038/ncomms2783, 2013.
- 32 Muscheler, R., Beer, J., and Vonmoos, M.: Causes and timing of the 8200yr BP event inferred
33 from the comparison of the GRIP ^{10}Be and the tree ring $\Delta^{14}\text{C}$ record, *Quaternary Sci*
34 *Rev*, 23, 2101-2111, <http://dx.doi.org/10.1016/j.quascirev.2004.08.007>, 2004a.
- 35 Muscheler, R., Beer, J., Wagner, G., Laj, C., Kissel, C., Raisbeck, G. M., Yiou, F., and Kubik, P.
36 W.: Changes in the carbon cycle during the last deglaciation as indicated by the
37 comparison of ^{10}Be and ^{14}C records, *Eart Planet Sc Lett*, 219, 325-340,
38 10.1016/s0012-821x(03)00722-2, 2004b.
- 39 Muscheler, R., Joos, F., Beer, J., Müller, S. A., Vonmoos, M., and Snowball, I.: Solar activity
40 during the last 1000yr inferred from radionuclide records, *Quaternary Sci Rev*, 26,
41 82-97, 10.1016/j.quascirev.2006.07.012, 2007.

- 1 Muscheler, R., Kromer, B., Björck, S., Svensson, A., Friedrich, M., Kaiser, K. F., and Southon,
2 J.: Tree rings and ice cores reveal ^{14}C calibration uncertainties during the
3 Younger Dryas, *Nat Geosci*, 1, 263-267, 10.1038/ngeo128, 2008.
- 4 Muscheler, R.: ^{14}C and ^{10}Be around 1650 cal BC, in: Time's up!: dating the Minoan eruption
5 of Santorini. Acts of the Minoan Eruption Chronology Workshop, Sandbjerg
6 November 2007, edited by: Warburton, D. A., Monographs of the Danish Institute at
7 athens, Danish Institute at Athens, Athens, 275-284, 2009.
- 8 Muscheler, R., and Heikkilä, U.: Constraints on long-term changes in solar activity from the
9 range of variability of cosmogenic radionuclide records, *Astrophysics and Space*
10 *Sciences Transactions*, 7, 355-364, 10.5194/astra-7-355-2011, 2011.
- 11 Muscheler, R., Adolphi, F., and Knudsen, M. F.: Assessing the differences between the IntCal
12 and Greenland ice-core time scales for the last 14,000 years via the common
13 cosmogenic radionuclide variations, *Quaternary Sci Rev*, 106, 81-87,
14 10.1016/j.quascirev.2014.08.017, 2014a.
- 15 Muscheler, R., Adolphi, F., and Svensson, A.: Challenges in ^{14}C dating towards the limit of
16 the method inferred from anchoring a floating tree ring radiocarbon chronology to
17 ice core records around the Laschamp geomagnetic field minimum, *Eart Planet Sc*
18 *Lett*, 394, 209-215, 10.1016/j.epsl.2014.03.024, 2014b.
- 19 Oeschger, H., Siegenthaler, U., Schotterer, U., and Gugelmann, A.: A box diffusion model to
20 study the carbon dioxide exchange in nature, *Tellus*, 27, 168-192, 10.1111/j.2153-
21 3490.1975.tb01671.x, 1975.
- 22 Pearce, N. J. G., Westgate, J. A., Preece, S. J., Eastwood, W. J., and Perkins, W. T.:
23 Identification of Aniakchak (Alaska) tephra in Greenland ice core challenges the 1645
24 BC date for Minoan eruption of Santorini, *Geochemistry, Geophysics, Geosystems*, 5,
25 Q03005, 10.1029/2003GC000672, 2004.
- 26 Pedro, J. B., Heikkilä, U. E., Klekociuk, A., Smith, A. M., van Ommen, T. D., and Curran, M. A.
27 J.: Beryllium-10 transport to Antarctica: Results from seasonally resolved
28 observations and modeling, *J Geophys Res-Atmos*, 116, n/a-n/a,
29 10.1029/2011jd016530, 2011a.
- 30 Pedro, J. B., Smith, A. M., Simon, K. J., van Ommen, T. D., and Curran, M. A. J.: High-
31 resolution records of the beryllium-10 solar activity proxy in ice from Law Dome, East
32 Antarctica: measurement, reproducibility and principal trends, *Clim Past*, 7, 707-721,
33 10.5194/cp-7-707-2011, 2011b.
- 34 Pedro, J. B., McConnell, J. R., van Ommen, T. D., Fink, D., Curran, M. A. J., Smith, A. M.,
35 Simon, K. J., Moy, A. D., and Das, S. B.: Solar and climate influences on ice core ^{10}Be
36 records from Antarctica and Greenland during the neutron monitor era, *Eart Planet*
37 *Sc Lett*, 355-356, 174-186, 10.1016/j.epsl.2012.08.038, 2012.
- 38 Pilcher, J. R., Baillie, M. G. L., Schmidt, B., and Becker, B.: A 7,272-year tree-ring chronology
39 for western Europe, *Nature*, 312, 150-152, 1984.
- 40 Raisbeck, G. M., Yiou, F., Fruneau, M., Loiseaux, J. M., Lieuvin, M., and Ravel, J. C.:
41 Cosmogenic $^{10}\text{Be}/^{7}\text{Be}$ as a probe of atmospheric transport processes, *Geophys Res*
42 *Lett*, 8, 1015-1018, 10.1029/GL008i009p01015, 1981.

- 1 Rasmussen, S. O., Andersen, K. K., Svensson, A. M., Steffensen, J. P., Vinther, B. M., Clausen,
2 H. B., Siggaard-Andersen, M. L., Johnsen, S. J., Larsen, L. B., Dahl-Jensen, D., Bigler,
3 M., Röthlisberger, R., Fischer, H., Goto-Azuma, K., Hansson, M. E., and Ruth, U.: A
4 new Greenland ice core chronology for the last glacial termination, *J Geophys Res*,
5 111, D06102, 10.1029/2005jd006079, 2006.
- 6 Reimer, P. J., Bard, E., Bayliss, A., Beck, J. W., Blackwell, P. G., Bronk Ramsey, C., Buck, C. E.,
7 Cheng, H., Edwards, R. L., Friedrich, M., Grootes, P. M., Guilderson, T. P., Haflidason,
8 H., Hajdas, I., Hatté, C., Heaton, T. J., Hoffmann, D. L., Hogg, A. G., Hughen, K. A.,
9 Kaiser, K. F., Kromer, B., Manning, S. W., Niu, M., Reimer, R. W., Richards, D. A.,
10 Scott, E. M., Southon, J. R., Staff, R. A., Turney, C. S. M., and van der Plicht, J.:
11 IntCal13 and Marine13 Radiocarbon Age Calibration Curves 0–50,000 Years cal BP,
12 *Radiocarbon*, 55, 1869-1887, 10.2458/azu_js_rc.55.16947, 2013.
- 13 Roth, R., and Joos, F.: A reconstruction of radiocarbon production and total solar irradiance
14 from the Holocene 14C and CO2 records: implications of data and model
15 uncertainties, *Clim Past*, 9, 1879-1909, 10.5194/cp-9-1879-2013, 2013.
- 16 Seierstad, I. K., Abbott, P. M., Bigler, M., Blunier, T., Bourne, A. J., Brook, E., Buchardt, S. L.,
17 Buizert, C., Clausen, H. B., Cook, E., Dahl-Jensen, D., Davies, S. M., Guillevic, M.,
18 Johnsen, S. J., Pedersen, D. S., Popp, T. J., Rasmussen, S. O., Severinghaus, J. P.,
19 Svensson, A., and Vinther, B. M.: Consistently dated records from the Greenland
20 GRIP, GISP2 and NGRIP ice cores for the past 104 ka reveal regional millennial-scale
21 $\delta^{18}O$ gradients with possible Heinrich event imprint, *Quaternary Sci Rev*, 106, 29-46,
22 <http://dx.doi.org/10.1016/j.quascirev.2014.10.032>, 2014.
- 23 Siegenthaler, U., Heimann, M., and Oeschger, H.: 14C variations caused by changes in the
24 global carbon cycle, *Radiocarbon*, 22, 177-191, 1980.
- 25 Sigl, M., Winstrup, M., McConnell, J. R., Welten, K. C., Plunkett, G., Ludlow, F., Buntgen, U.,
26 Caffee, M., Chellman, N., Dahl-Jensen, D., Fischer, H., Kipfstuhl, S., Kostick, C.,
27 Maselli, O. J., Mekhaldi, F., Mulvaney, R., Muscheler, R., Pasteris, D. R., Pilcher, J. R.,
28 Salzer, M., Schupbach, S., Steffensen, J. P., Vinther, B. M., and Woodruff, T. E.:
29 Timing and climate forcing of volcanic eruptions for the past 2,500 years, *Nature*,
30 523, 543-549, 10.1038/nature14565
31 [http://www.nature.com/nature/journal/vaop/ncurrent/abs/nature14565.html#supplement](http://www.nature.com/nature/journal/vaop/ncurrent/abs/nature14565.html#supplementary-information)
32 [ary-information](http://www.nature.com/nature/journal/vaop/ncurrent/abs/nature14565.html#supplementary-information), 2015.
- 33 Southon, J.: A First Step to Reconciling the GRIP and GISP2 Ice-Core Chronologies, 0–14,500
34 yr B.P, *Quaternary Res*, 57, 32-37, 10.1006/qres.2001.2295, 2002.
- 35 Spurk, M., Leuschner, H. H., Baillie, M. G. L., Briffa, K. R., and Friedrich, M.: Depositional
36 frequency of German subfossil oaks: climatically and non-climatically induced
37 fluctuations in the Holocene, *The Holocene*, 12, 707-715,
38 10.1191/0959683602h1583rp, 2002.
- 39 Stuiver, M., Braziunas, T. F., Grootes, P. M., and Zielinski, G. A.: Is There Evidence for Solar
40 Forcing of Climate in the GISP2 Oxygen Isotope Record?, *Quaternary Res*, 48, 259-
41 266, 10.1006/qres.1997.1931, 1997.

- 1 Stuiver, M., Reimer, P. J., Bard, E., Beck, J. W., Burr, G. S., Hughen, K., Kromer, B., McCormac,
2 F. G., Van der Plicht, J., and Spurk, M.: INTCAL98 radiocarbon age calibration, 24000-
3 0 cal BP, *Radiocarbon*, 40, 1041-1083, 1998.
- 4 Svensson, A., Andersen, K. K., Bigler, M., Clausen, H. B., Dahl-Jensen, D., Davies, S. M.,
5 Johnsen, S. J., Muscheler, R., Parrenin, F., Rasmussen, S. O., Röthlisberger, R.,
6 Seierstad, I., Steffensen, J. P., and Vinther, B. M.: A 60 000 year Greenland
7 stratigraphic ice core chronology, *Clim Past*, 4, 47-57, 10.5194/cp-4-47-2008, 2008.
- 8 Vinther, B. M., Clausen, H. B., Johnsen, S. J., Rasmussen, S. O., Andersen, K. K., Buchardt, S.
9 L., Dahl-Jensen, D., Seierstad, I. K., Siggaard-Andersen, M. L., Steffensen, J. P.,
10 Svensson, A., Olsen, J., and Heinemeier, J.: A synchronized dating of three Greenland
11 ice cores throughout the Holocene, *J Geophys Res*, 111, D13102,
12 10.1029/2005jd006921, 2006.
- 13 Vonmoos, M., Beer, J., and Muscheler, R.: Large variations in Holocene solar activity:
14 Constraints from ^{10}Be in the Greenland Ice Core Project ice core, *J Geophys Res*, 111,
15 A10105, 10.1029/2005ja011500, 2006.
- 16 Yiou, F., Raisbeck, G. M., Baumgartner, S., Beer, J., Hammer, C., Johnsen, S., Jouzel, J., Kubik,
17 P. W., Lestringuez, J., Stiévenard, M., Suter, M., and Yiou, P.: Beryllium 10 in the
18 Greenland Ice Core Project ice core at Summit, Greenland, *J Geophys Res*, 102,
19 26783, 10.1029/97jc01265, 1997.

20

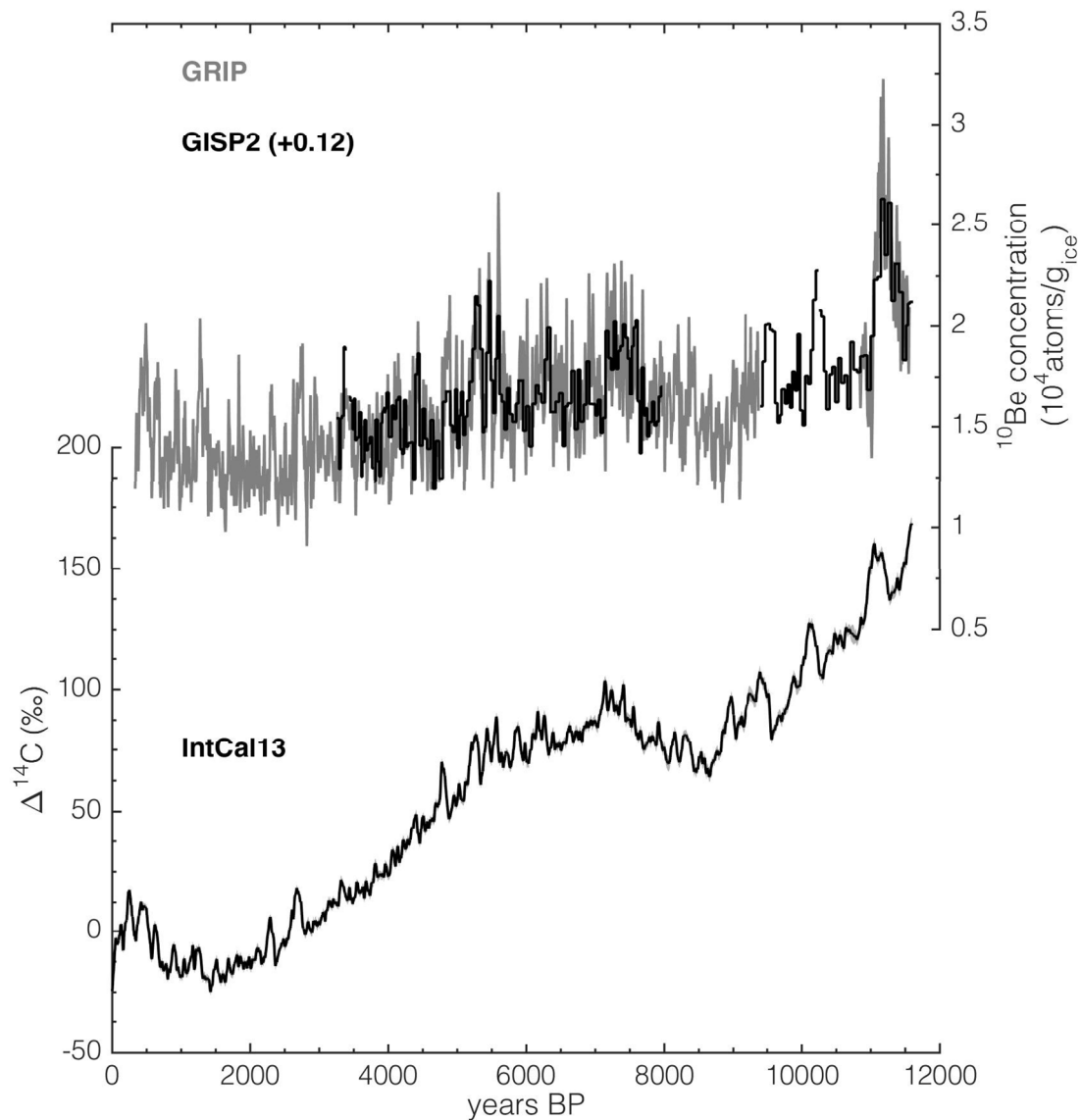
21

1 Table 1. Performed carbon cycle sensitivity experiments. All percentage values refer to the
2 control simulation under pre-industrial conditions.

	Control	S1	S2	S3	S4
Air/Sea Exchange	100 %	150 %	50 %	100 %	100 %
Ocean ventilation	100 %	100 %	100 %	150 %	50 %

3

4



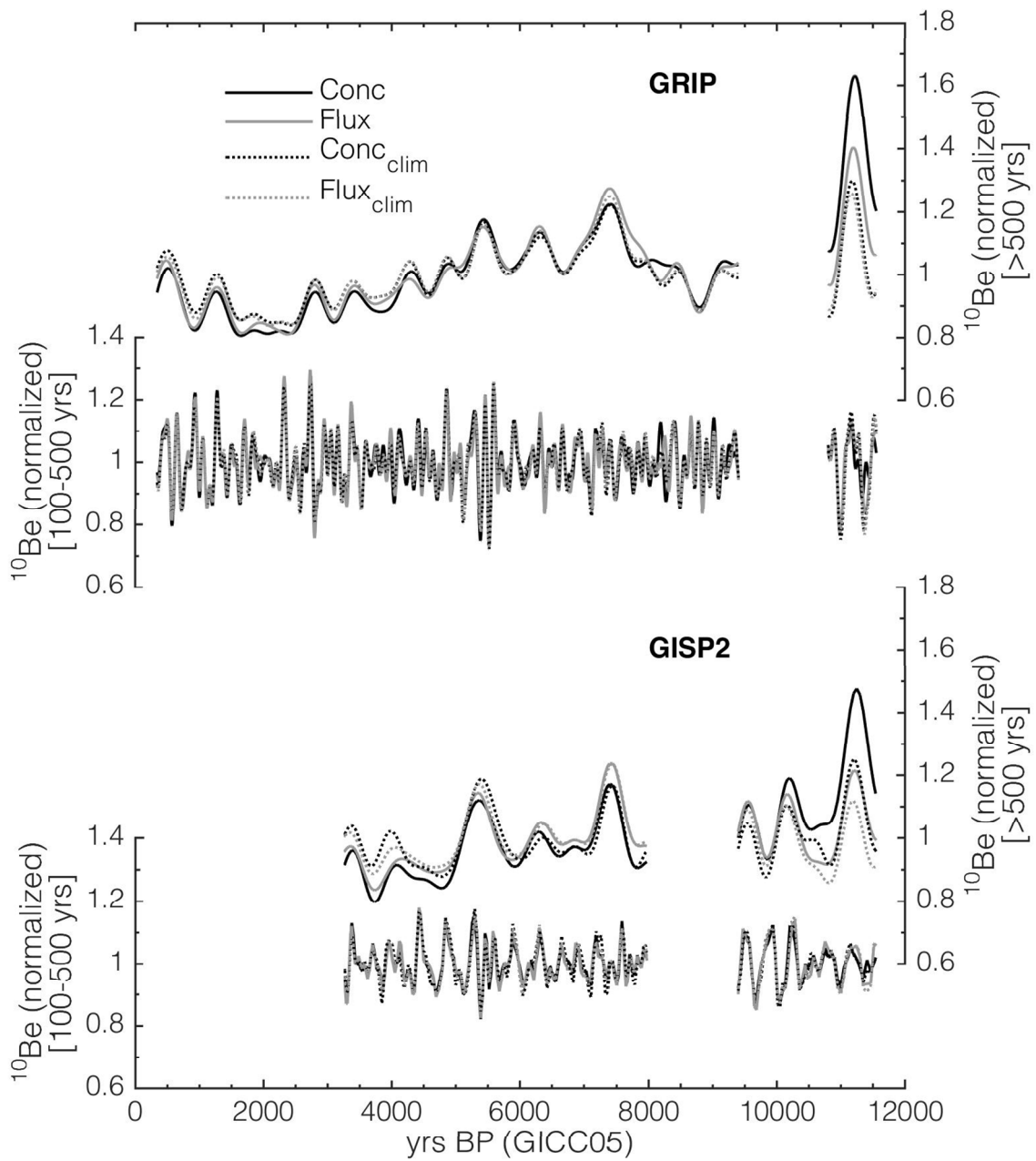
1

2 Figure 1: *Top*: GRIP (grey, Vonmoos et al., 2006) and GISP2 (black, Finkel and Nishiizumi,
 3 1997) Holocene ^{10}Be concentrations. The GRIP ^{10}Be record is smoothed by a 61-pt binomial
 4 filter (see Vonmoos et al., 2006). The GISP2 ^{10}Be record has been shifted by
 5 $+0.12 \cdot 10^4$ atoms/g to correct for a difference in the mean of the GRIP and GISP2 ^{10}Be
 6 records. *Bottom*: Atmospheric $\Delta^{14}\text{C}$ as reconstructed from tree rings (Reimer et al., 2013 and
 7 references therein).

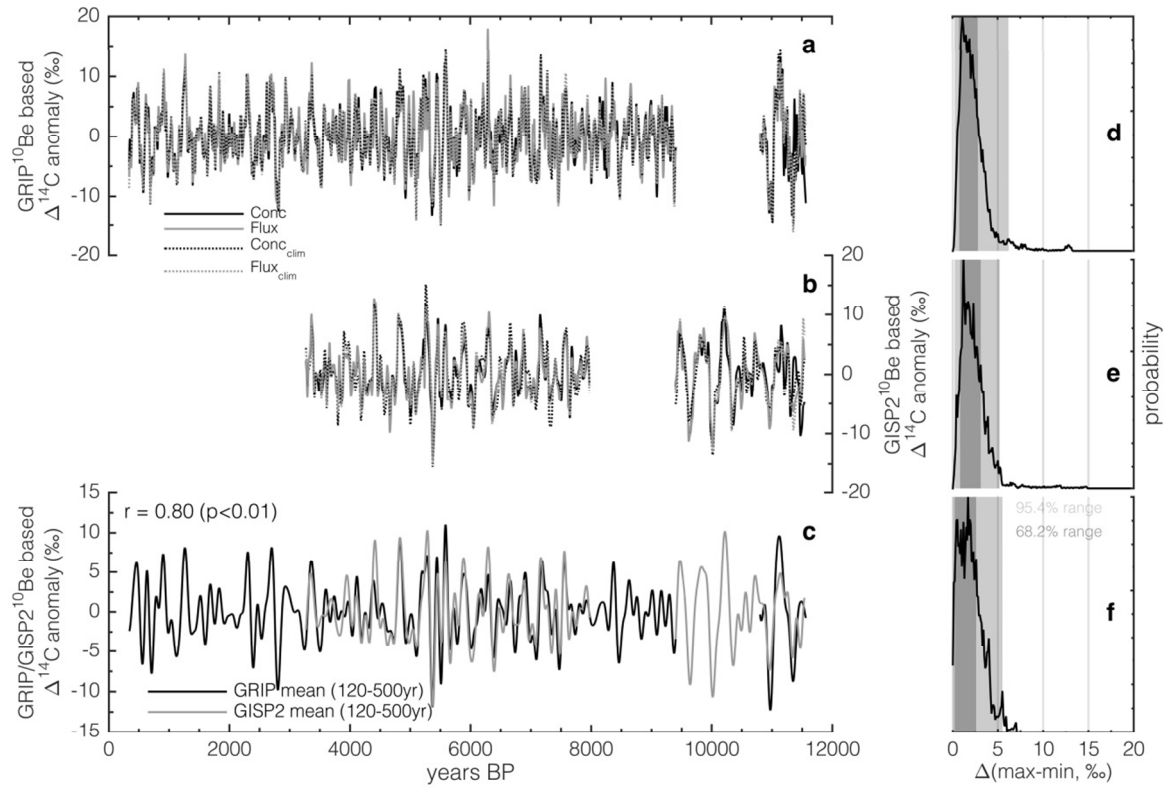
8

9

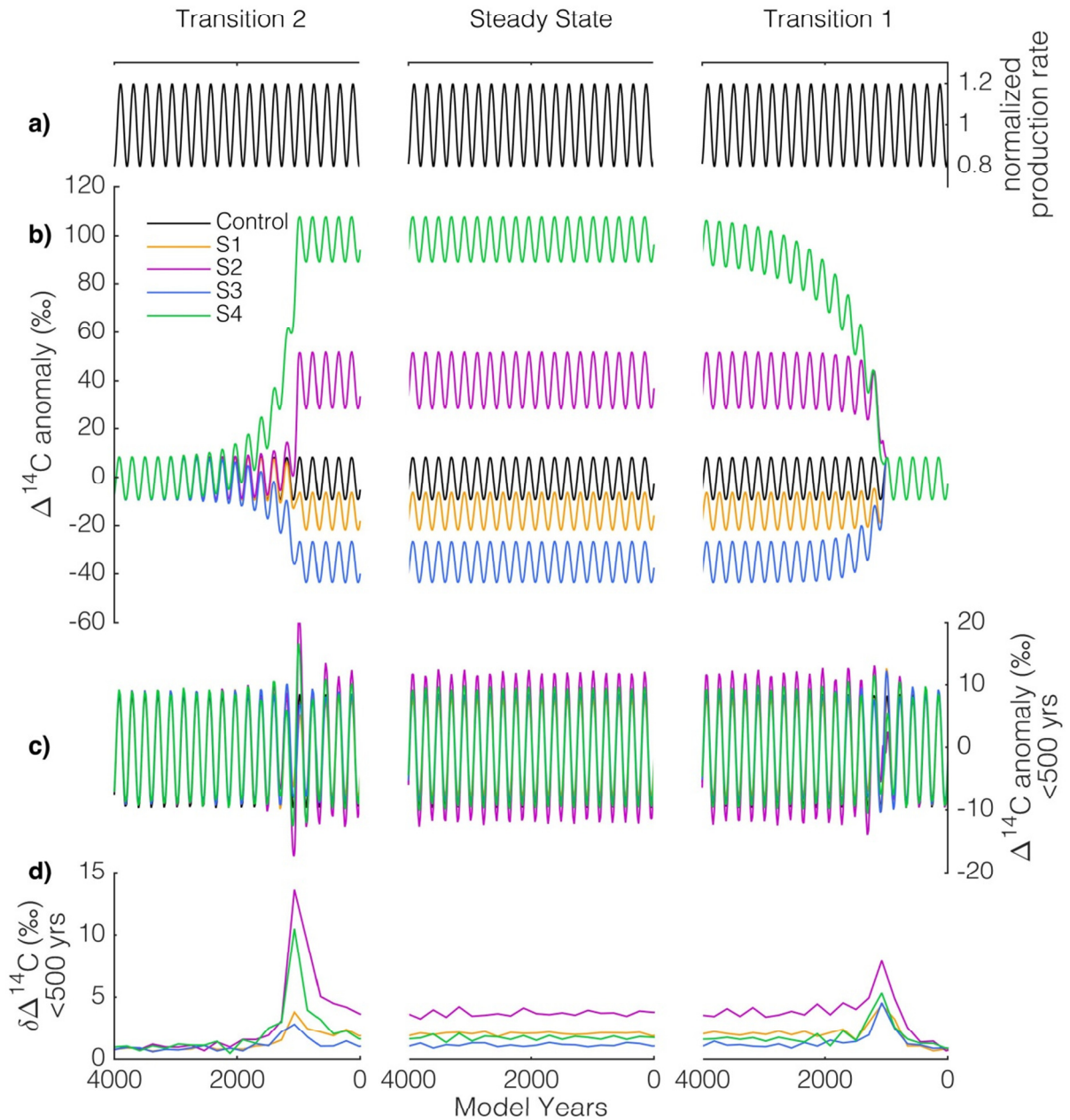
10



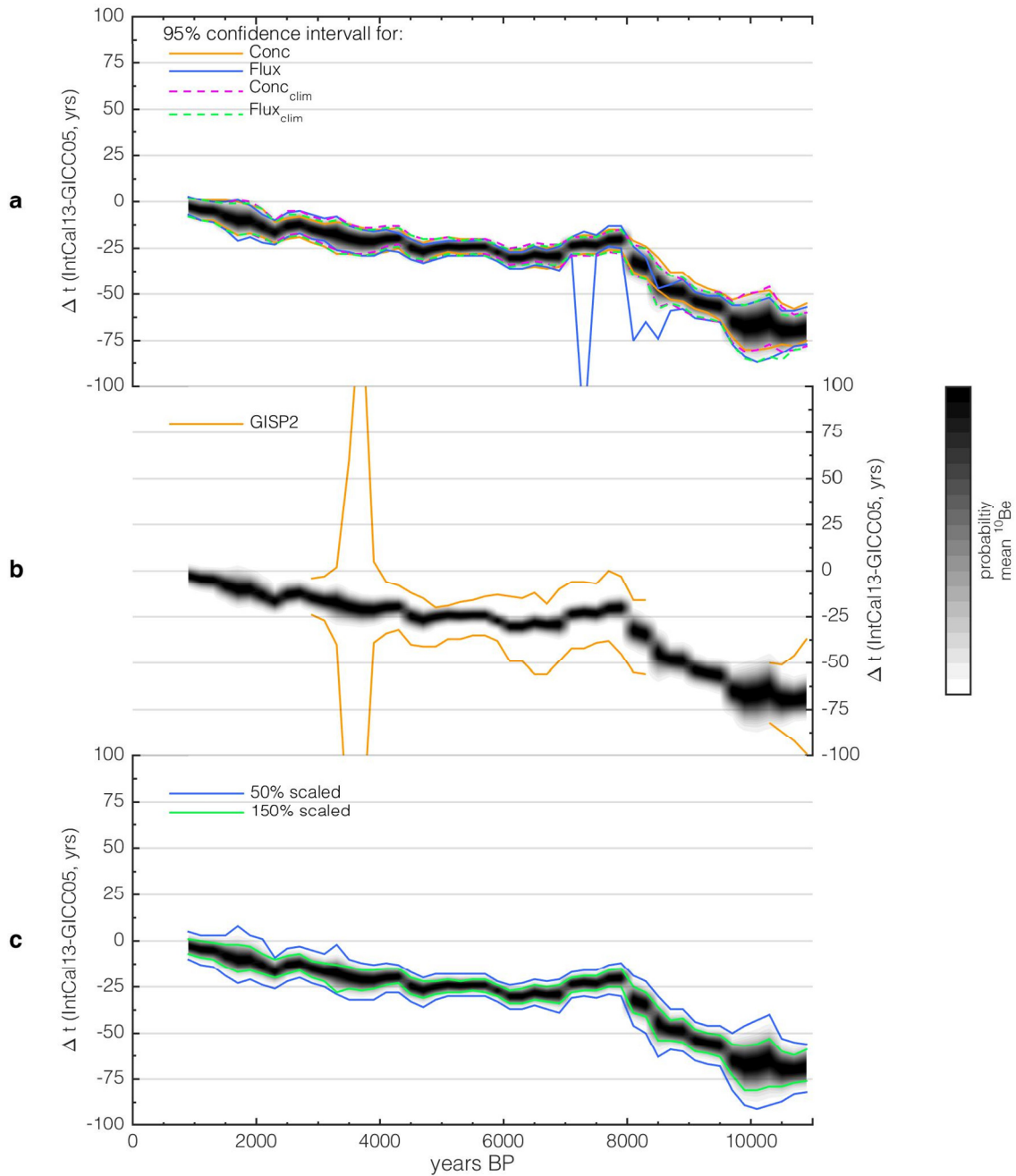
1
 2 Figure 2: Comparison of ^{10}Be fluxes and concentrations over the Holocene. Solid black and
 3 grey curves denote ^{10}Be concentrations and fluxes, respectively. Dotted lines refer to the
 4 “climate corrected” (see text) versions of concentrations and fluxes with similar colour
 5 coding as solid lines. The top two panels show GRIP ^{10}Be for variations on time scales longer
 6 (top) than 500 years, and for wavelengths between 100-500 years (below). The 100 year cut-
 7 off has been applied for clarity of the figure. The bottom two panels show GISP2 ^{10}Be for the
 8 same wavelengths as for GRIP.



1
2 **Figure 3. Centennial (<500 years) $\Delta^{14}\text{C}$ variations modelled from GRIP and GISP2 ^{10}Be data.**
3 **Panels a and b show the modelled $\Delta^{14}\text{C}$ variations from ^{10}Be concentrations (solid black),**
4 **fluxes (solid grey), “climate corrected” concentrations (dotted black), and “climate corrected”**
5 **fluxes (dotted grey) for the GRIP (a) and GISP2 (b) ^{10}Be records. Panels d and e on the right**
6 **side depict the probability density functions for the maximum $\Delta^{14}\text{C}$ difference between**
7 **curves shown in panels a and b, respectively. Panel c shows the mean of all GRIP (black) and**
8 **GISP2 (grey) ^{10}Be based $\Delta^{14}\text{C}$ anomalies shown in panels a and b, respectively. Panel f**
9 **shows the corresponding probability density function of their maximum $\Delta^{14}\text{C}$ differences. For**
10 **this comparison both ice core records have been band-pass filtered [120 – 500 years] to**
11 **minimize inconsistencies arising from their different sampling resolution. The correlation**
12 **between the GRIP and GISP2 records is given in panel c together with its p-value.**
13



1
2 **Figure 4.** Carbon cycle sensitivity experiments. a) Normalized ^{14}C production rate input to
3 the model. b) Modelled $\Delta^{14}\text{C}$ anomaly. c) Centennial (<500 year) anomalies of modelled
4 $\Delta^{14}\text{C}$ shown in panel b. d) differences in the centennial $\Delta^{14}\text{C}$ variations (panel c) from the
5 control run. All model runs and panels are shown for the transition from preindustrial to
6 perturbed conditions (transition 1, right), steady state of the perturbed conditions (steady
7 state, middle), and the transition back to preindustrial carbon cycle conditions (transition 2,
8 left). See also section 2.4.1.

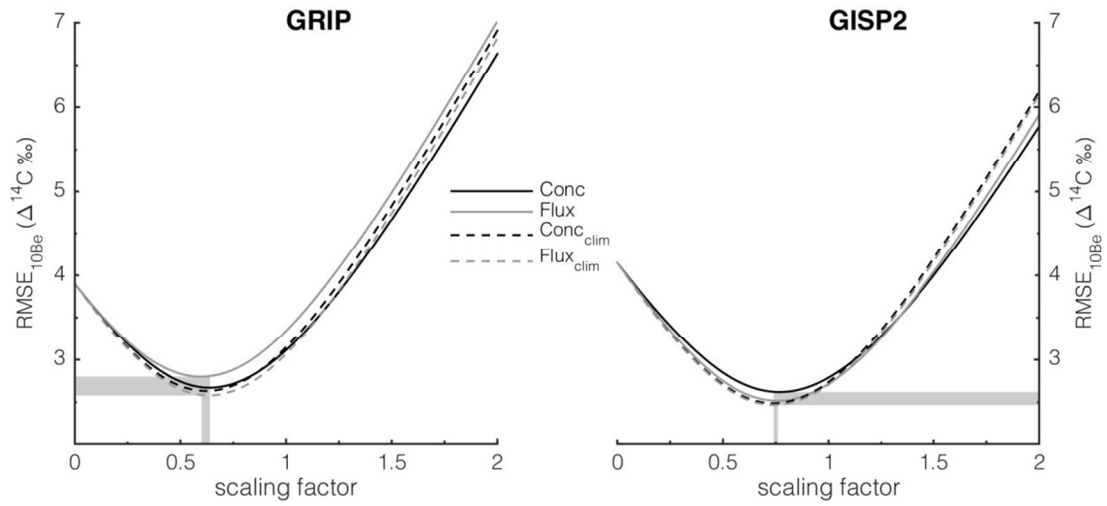


1

2 **Figure 5.** Probability distributions for IntCal13-GICC05 timescale differences ($P_{scaled}(t_s)$,
 3 see section 2.1) for each 1,000-year window based on the mean of GRIP ^{10}Be concentrations,
 4 fluxes, and their climate corrected versions (grey-scale patches in all panels). The gap in the
 5 GRIP ^{10}Be record between 9,400 and 10,800 BP has been filled with data from the GISP2 ice
 6 core. Each probability distribution is centred on the mean age of the investigated window. a)
 7 Comparison to 95% probability intervals based on GRIP ^{10}Be concentrations (solid orange),
 8 fluxes (solid blue) and their “climate corrected versions (dashed pink and green lines). b)
 9 Comparison to 95% confidence intervals based on the mean of GISP2 ^{10}Be concentrations,

1 fluxes, and their climate corrected versions. Results for GISP2 are only shown for periods
2 where it has not been used to fill the gap in the GRIP record. c) Comparison to results based
3 on a different scaling (factors of 0.5 and 1.5 shown as blue and green lines, respectively) of
4 the GRIP ¹⁰Be record.

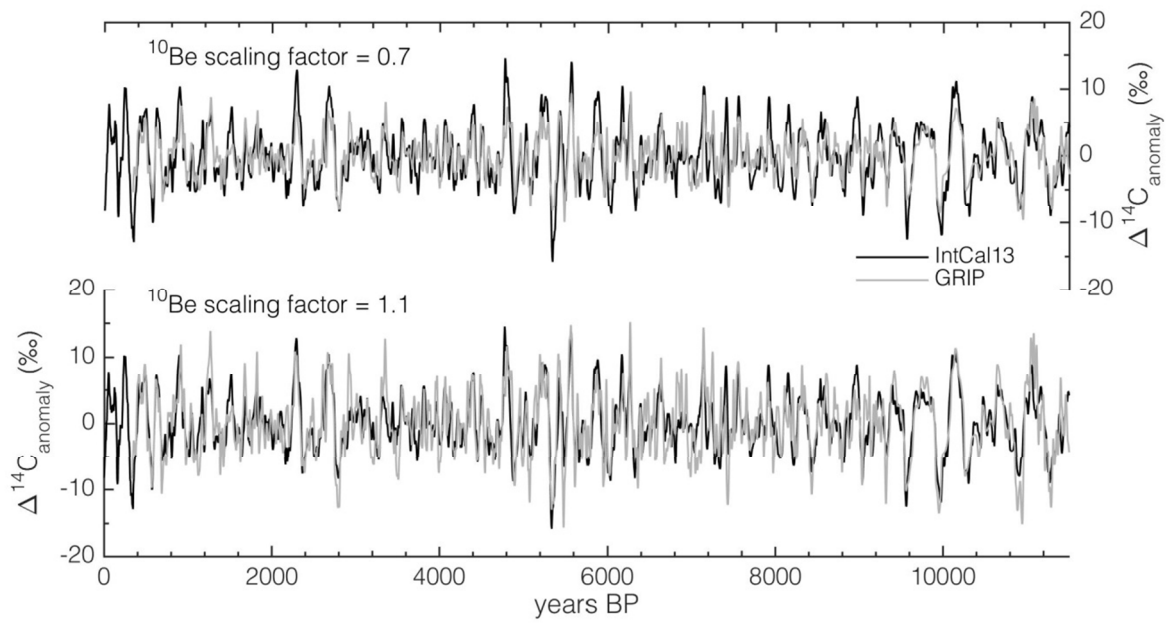
5



1

2 Figure 6. Rooted mean square error ($RMSE_{10Be}$, see text) of synchronized centennial IntCal13
 3 and ^{10}Be -based $\Delta^{14}C$ variations as a function of different ^{10}Be -scaling factors ($^{14}C:^{10}Be$
 4 ratios). Results for the different versions of the GRIP ^{10}Be record are shown on the left, while
 5 GISP2 ^{10}Be -based results are shown on the right.

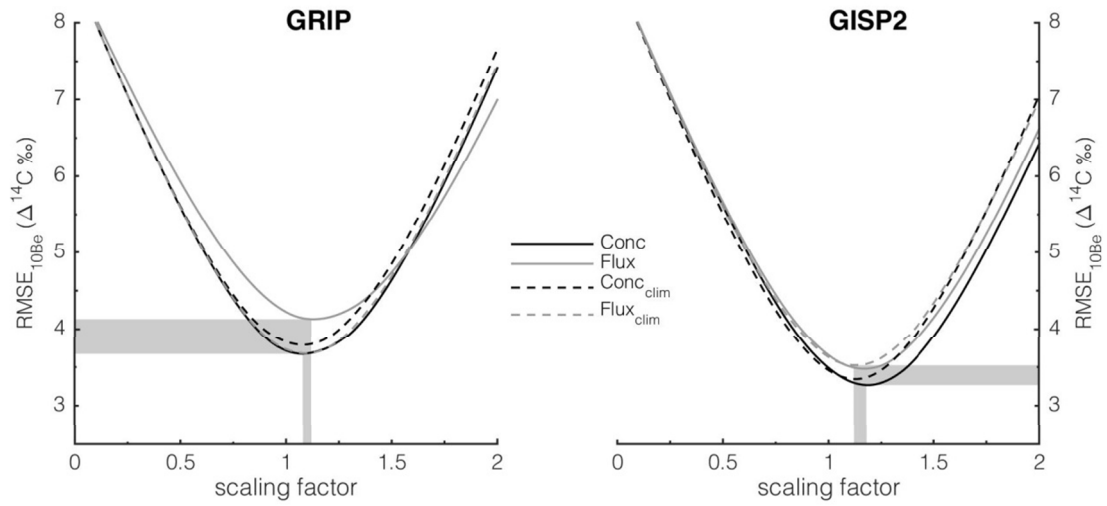
6



1

2 Figure 7. Comparison of synchronized tree-ring (black) and ice core (grey) based $\Delta^{14}\text{C}$
 3 anomalies for $^{14}\text{C}:^{10}\text{Be}$ ratios of 0.7 (top) and 1.1 (bottom).

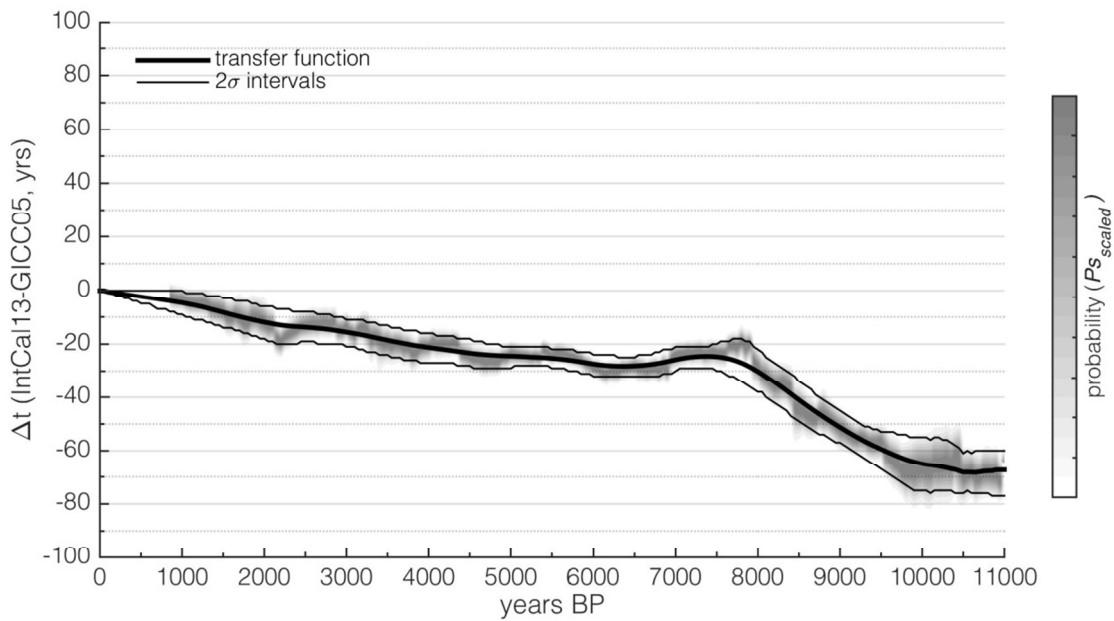
4



1

2 Figure 8. Rooted mean square error (RMSE_{10Be}) of IntCal13 Δ¹⁴C and ¹⁰Be based Δ¹⁴C
 3 records from GRIP (left) and GISP2 (right) for different scalings of the ¹⁰Be based data after
 4 synchronization. The RMSE_{10Be} has been calculated for binned data (bin size = 2.5 ‰, see
 5 text) taking IntCal Δ¹⁴C errors into account.

6



1

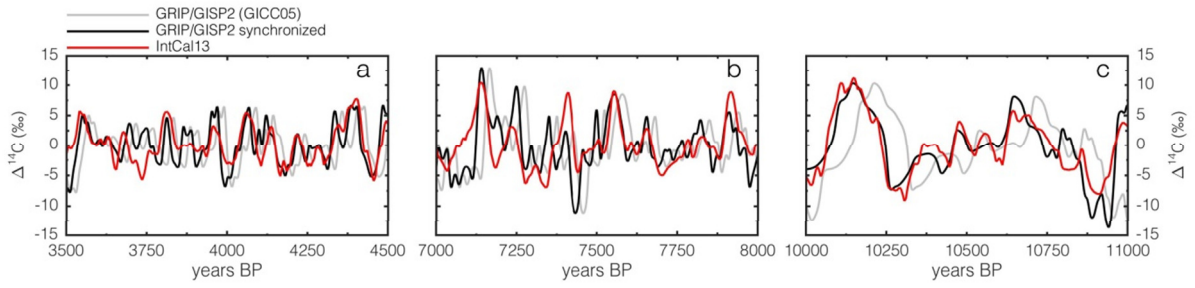
2 Figure 9. IntCal13-GICC05 age transfer function (thick black line) and its 2σ confidence

3 intervals (thin black lines) based on the probability distributions ($P_{scaled}(t_s)$, grey shading)

4 obtained from comparing the GRIP ^{10}Be -based $\Delta^{14}\text{C}$ (mean of concentration, flux and climate

5 corrections) and IntCal13 $\Delta^{14}\text{C}$ records.

6

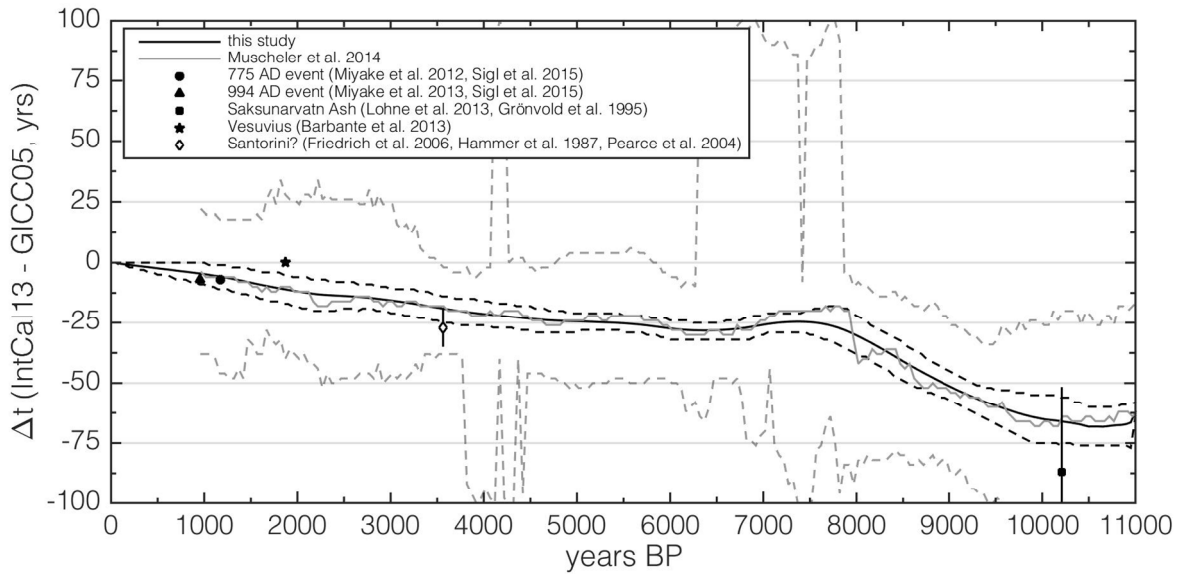


1

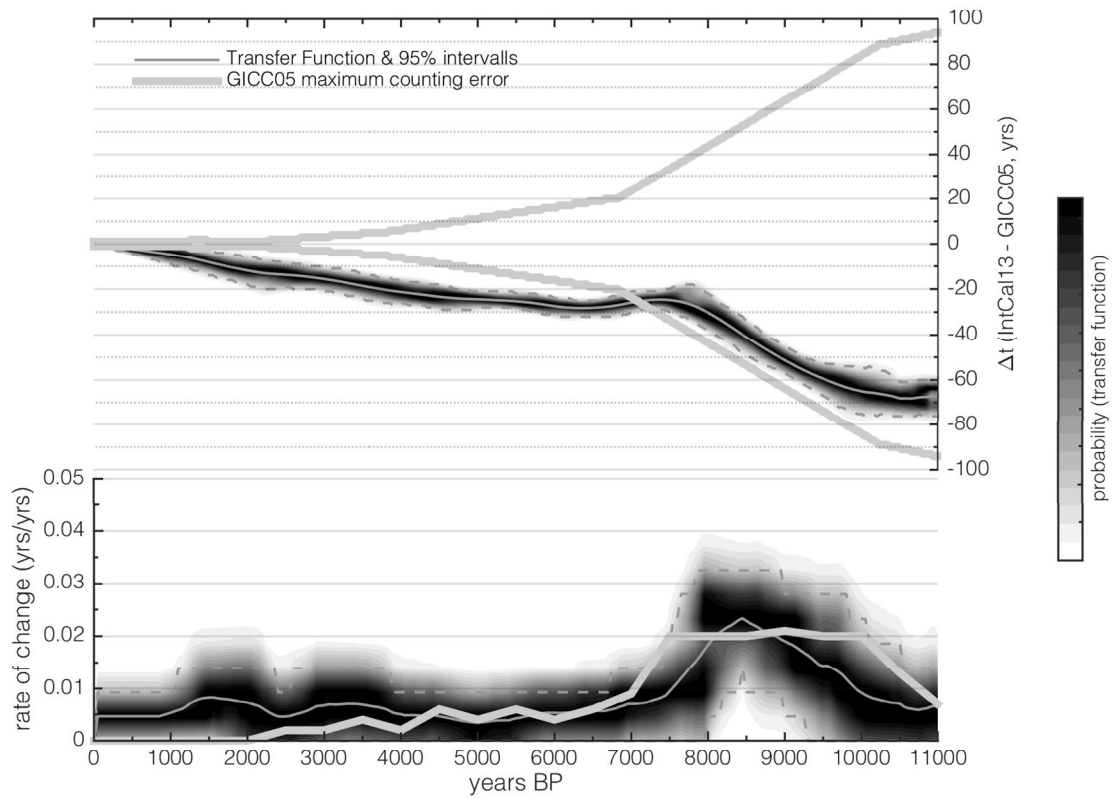
2 **Figure 10. GRIP/GISP2 ^{10}Be based $\Delta^{14}\text{C}$ before (grey) and after (black) synchronization to**
 3 **IntCal13 (red) for the sections a) 3,500-4,500 years BP, b) 7,000-8,000 years BP, c) 10,000-**
 4 **11,000 years BP.**

5

6



1
2 Figure 11. Comparison of the derived IntCal13-GICC05 timescale transfer function (black
3 lines, this study) to the results by Muscheler et al. (2014, grey lines), and independent age
4 markers that have been linked independently to the IntCal13 and GICC05 timescales at high
5 precision (symbols). The results of this study and Muscheler et al. are shown with their
6 respective 95 % confidence intervals (dashed lines). The independent age markers are plotted
7 as the difference between their estimated ages based on radiocarbon dating (Saksunarvatn
8 Ash, Santorini), historical documents (Vesuvius) and dendrochronology (775 and 994 AD
9 events), and their respective GICC05-ages. The plotted 1σ error bars largely reflect
10 uncertainties in the radiocarbon-dating and calibration of the Saksunarvatn Ash (Lohne et al.,
11 2013) and the Santorini eruption (Friedrich et al., 2006). Note that the identification of the
12 Santorini tephra in ice cores has been challenged based on its geochemistry (Pearce et al.,
13 2004).
14



1

2 Figure 12. Top: Comparison of the derived IntCal13-GICC05 transfer function (thin grey
 3 lines and shading, dashed lines denote the 95% confidence interval) to the GICC05 maximum
 4 counting error (bold grey lines). Bottom: Same as above but expressed as the rate of change
 5 (yrs/yrs) of the GICC05 maximum counting error and the derived timescale transfer function.

6